UNIVERSIDAD DE INGENIERÍA Y TECNOLOGÍA UTEC

Energy Engineering

PERFORMANCE EVALUATION OF SILVER- BASED NANOMATERIALS ENHANCED WITH FULLERENES AS CATHODES FOR FLEXIBLE ZINC-AIR BATTERIES

Thesis for the Bachelor Degree in Energy Engineering

Danae Ariana Chipoco Haro

Student ID: 201510107

Advisor

Juan Carlos Rodríguez Reyes

Lima – Peru

April 2020

The thesis

PERFORMANCE EVALUATION SILVER-BASED NANOMATERIALS ENHANCED WITH FULLERENES AS CATHODES FOR FLEXIBLE ZINC-AIR BATTERIES

Has been approved

[Nombres y apellidos del Presidente de Jurado]

Juan Carlos Rodríguez Reyes

[Nombres y apellidos del Tercer jurado]

Dedication:

To God, my Lord, my strength and rest.

To my father, for being an example of prudence. To my mother, for the wisdom and confidence she has always transmitted me. To them both, for their care, for supporting my dreams even though they did not understand them, for the guidance, and for their unconditional love. To my grandmother, for being a silent companion, a unique support, a withstanding professional and, overall, a model. To my brother, with whom I shared many thoughts and thought me through silence. To my family, for their kindness and for always backing me.

To my Master, who showed me the Jedi path.

To all my friends. To the loyal ones which stayed by my side even though life took as through different paths. To my project partner, with whom a shared dream took us through many adventures and thought me many lessons. To the ones with whom I shared deep conversations and fandom analysis. To my classmate since school, for her kindness and complicity. To my little sister, for all the things she thought me without knowing, for all the friendly games, happy memories and her support on the most difficult moments of my journey.

To my teachers and administrative staff at UTEC, who supported me during these years, who believed in me long before I did, and went beyond what their duty dictated.

To the land witness of my birth, my growth and the society that forged my personality. Because, despite all the trouble time we may be going through, I believe in our strength to overcome the differences and join together to build a dreamed Peru.

Acknowledgments:

First, I would like to thank Ph.D. Juan Carlos Rodriguez-Reyes, who guided me throughout the development of the thesis as an advisor and mentor, for introducing me to his research group and colleagues who helped me in many ways in this work, for his commitment in my professional and personal growth, for his support and comprehension in difficult times, for being a model of a researcher, professor, and ethic person, for the kindness he has always shown to me, and for being my Master.

I would also like to thank Dr. Adolfo de la Rosa Toro for allowing me to work with his research group, facilitating equipment and materials for the different electroanalytical tests, and Dr. Angélica Baena, for allowing me to work in the facilities under her supervision.

Specially, I would like to thank Ph.D. Julio Valdivia for his support by allowing me to use the facilities under his supervision and Ph.D. Julien Noel, for the economic support for the study and his guidance during these five years of undergraduate studies.

A very special gratitude goes to Luis Palomino, for his guidance in the use of equipment and techniques for nanoparticles synthesis and life lessons he gave me. Also, to Antony Bazán, Rey Fernández, Yuri Ccallocunto and Ana Luz Tupa for their guidance in the use of equipment for electroanalytical tests, the help in the interpretation of the obtained data and the support during the study.

With a special mention and affection to Karinna Visurraga, Luz Pérez, Giuliana Travi and Jesenia Zapata, for their administrative and logistical support, and the kind guidance throughout the project. Also, to Sheyla Chero and Carsten Benndorf, for the useful discussion and help in the XPS measurements and Mario Carbajal, Flor Granda and Andrea Aranda for their logistical help in the laboratory. As well as Ximena Guardia, for her help in the writing of the thesis and comprehension.

I am also grateful to José Ruiz, Rocío Hoyos and Vanessa Quispe for the useful discussions and lessons on electrochemistry.

And finally, last but by no means least, also to everyone in the Research Group of Juan Carlos Rodriguez-Reyes (UTEC) and Research Group from Applied Electrochemistry (UNI) for welcoming me at the research group.

TABLE OF CONTENT

Pág.

ABBREVIATION INDEX

CNT	carbon nanotubes
CV	cyclic voltammetry
GDL	gas diffusion layer
NP	nanoparticle
OCP	open circuit potential
OER	oxygen evolution reaction
ORR	oxygen reduction reaction
PHF	hydroxyl fullerene
SPR	surface plasmon resonance
UV-vis	ultraviolet and visible absorption spectroscopy
XPS	X-ray photoelectron spectroscopy

TABLE INDEX

Pág.

FIGURE INDEX

Pág.

ANNEX INDEX

ABSTRACT

Metal-air batteries are characterized by a high energy density with relatively simple and safe chemistry which makes them suitable for many applications, especially the ones requiring flexibility. These energy storage devices consist of one metal electrode, an air electrode, which enhance the oxygen evolution and oxygen reduction reactions (OER and ORR, respectively), and an electrolyte. The air electrode is lighter than most metal electrodes present in batteries; therefore, these batteries have a high energy density. However, the most critical problem this technology faces involves the air electrode design, especially because of the requirement of a bifunctional catalyst for OER and ORR.

Here, the enhancement of the catalytic activity of silver nanoparticles impregnated on carbon nanotubes (CNT) for OER and ORR using polyhydroxy fullerene (PHF) is discussed, as well as the methodology needed for an experimental demonstration of this hypothesis. This study contributes to the worldwide efforts of the scientific community to develop flexible, small and light batteries and may be a starting point in the use of PHF for this application.

Keywords: Flexible air electrode, Zn-air batteries, silver nanoparticles synthesis, PHF, cyclic voltammetry, XPS, galvanostatic charge-discharge, UV-vis.

INTRODUCTION

"The important thing is not to stop questioning."

- *Albert Einstein*

Up to 2020, an increase in more than 50% in wearable devices acquisitions in comparison to 2016 is expected [1]. This market trend shows the interest of big industries in the development of flexible components for these devices, including energy storage devices such as batteries. There has been a great advance in this field, but there are more things that can be done.

Among the many types of energy-storage devices evaluated as candidates to achieve the flexibility needed, metal-air batteries have become very promising due to their high energy density with a relatively simple and safe chemistry [2]. There are plenty of metals suitable for this application, being the most common lithium, magnesium, aluminum and zinc [3].

This study focuses on zinc-air batteries because of their high energy density [2],low price [4], [5], and abundance in the continental crust [6], especially in Peru as the third zinc exporter worldwide [4].Even though the scientific work on the field is considerable, there are still some challenges to overcome. One of the most critical problem this technology faces involves the air electrode design, especially because of the requirement of a bifunctional catalyst for oxygen reduction reaction (ORR) and oxygen evolution reaction (OER) [7]. Therefore, this thesis explores the theory behind the use of different materials as flexible air cathodes to evaluate their catalytic activity and the resulting impact they may have on the performance of flexible Zn-air batteries. Specifically, the materials explored will be carbon buckypaper impregnated with silver nanoparticles and silver nanoparticles with PHF. The methods evaluated for synthesizing silver nanoparticles were the Frens method and one developed by the groups of Juan Carlos Rodriguez-Reyes at UTEC and Vijay Krishna at

Cleveland Clinic, using PHF as reducing agent, which size determination could be estimated using UV visible light spectroscopy. The air cathode is proposed to be built by the impregnation of these materials over carbon nanotube (CNT) buckypaper which acts as current collector and support. The characterization proposed for these electrodes is X-ray photoelectron spectroscopy, while the catalytic activity towards OER and ORR can be determined by cyclic voltammetry and galvanostatic charge-discharge tests will prove its stability over time. The literature review showed PHF as a stabilizer for noble-metal nanoparticles, moreover, it is hypothesized that PHF can also be used as reducing agent in the synthesis of noble-metal nanoparticles, more specifically, silver nanoparticles, thus, enhancing its catalytic activity towards ORR and OER.

Scope

The present work involves the theoretical comparison of the performance of different nanoparticles-based materials as flexible cathodes for Zn-air batteries and the establishment of a suitable method for the experimental evaluation of these flexible cathodes looking forward to its further application.

The proposed methodology includes the specifications of the synthesis of silver nanoparticles and its further impregnation over CNT buckypapers for the flexible cathode building, as well as the characterization techniques and the electrochemical tests for the performance evaluation of the cathodes in terms of catalytic activity and stability over time. The selected characterization techniques were X-ray spectroscopy (XPS) for the characterization of the air cathode and UV-visible absorption spectroscopy (UV-vis) for determining the size of the silver nanoparticles synthesized. The electrochemical tests proposed for the performance evaluation are open circuit potential, cyclic voltammetry and galvanostatic charge-discharge test. Other techniques and methods are excluded for the analysis of this work. Among them, polarization curves and rotating disk electrode, an electrode that, as its name suggest, is in constant motion to control and determine the reactant transportation in the electrode's surroundings, which allows the analysis of electron-transfer

kinetics. The test of these electrodes in a battery prototype as well as an economic evaluation and marked comparison are out of the scope of this study.

The presented work is done in the Research Group of Juan Carlos Rodriguez-Reyes at the Universidad de Ingeniería y Tecnología (UTEC), with the support of the Research Group from Applied Electrochemistry of the Universidad Nacional de Ingeniería (UNI) in charge of Adolfo de la Rosa Toro Gómez.

Background information

There are plenty of synthesis and assembly methods for flexible air electrodes found in the literature [3]. However, the most direct and simplest method is to grow a gas diffusion and catalytic layer over a current collector [8]. The materials most widely used have been carbon-based current collectors due to the stability of their structures, high conductivity and light-weight. However, other materials like nano-silver ink for printing [9], titanium [10] and stainless steel mesh [11], have also been used with good battery performances. For example, the stainless steel mesh used showed more binding capability to the catalysts than carbon-based materials due to its mechanical strength [12]. The advantages and disadvantages that each current collector gives have been an important part of some studies. In this work, carbon nanotubes (CNT) in the form of buckypaper is proposed as current collectors.

One of the limiting factors in the development of Zn-air batteries is the lack of efficient bifunctional catalysts for oxygen evolution and reduction reactions in the air cathode [13]. Therefore, the scientific community has been working on the synthesis of new stable catalysts. Noble-metal oxides are highly active for OER and have a good metallic conductivity, however, they are expensive in comparison to other materials. There have been also considered transition metals oxides, which are not as expensive as the noble-metal oxides and possess semiconducting properties [2]. Many of these materials are combined along with different synthesis methods in the search of more efficient materials for the air cathode of Zn-air batteries.

Silver is a noble metal which has been reported to be an effective catalyst for ORR due to the reduction reaction involving four electrons (as will be described below), similar to platinum catalysts. However, silver presents difficulties in the adsorption of oxygen molecules, therefore, scientists usually combine this noble metal with other materials to improve the catalytic activity of silver [14]. There are many synthesis methods available for preparing silver particles and impregnating them over the conductor layer and gas diffusion layer (GDL), like the hydrothermal method, pulsed layer deposition method, reduction, among others. A summary of the performances of some Zn-air batteries developed using Ag-based catalysts in the air cathode synthesized with different methods, can be found on ANNEX 1.

Some studies developed by J. Guo and collaborators used $NaBH_4$ and sodium citrate for the synthesis of catalysts containing silver for reduction activity in alkaline media with notable results. First, they developed an Ag/C catalyst using a citrate-protecting method which ORR activity was found to proceed through a four-electron pathway [15]. Then, they developed a Co-based phthalocyanines on Ag nanoparticles supported on carbon which ORR activity was higher than Ag catalysts band Co-based phthalocyanines on carbon [16].

Furthermore, Y. Jin and collaborators synthesized a Ag-Cu alloy using sodium citrate as complexing agent. The Zn-air battery developed with this catalyst exhibited an open circuit voltage of 1.49 V and power density of 86.5 mW cm^{-2} at 100 mA cm^{-2}, and a round efficiency of 56.4% at 20 mA cm^{-2} [17].

This study will use the synthesis protocols developed by Research Group of Juan Carlos Rodriguez-Reyes [18], [19], which used sodium citrate as reducing agents for silver nanoparticles synthesis. Moreover, this study will use polyhydroxy fullerene (PHF) as surfactant and to enhance the catalytic activity of the silver nanoparticles for OER and ORR. These synthesis methods, to the best of the author's understanding, have not been used for this application before.

Justification

Modern electronics is a developing field that has reached a point in which the competition on low cost and improved performance is ever-increasing. Therefore, nowadays companies are focusing on other attributes to increase the value of their products, being flexibility one that stands out among others due to the variety of fields requiring this property [20]. These fields include, but are not limited to, wearables for commercial and biomedical applications [21], [22], with an increasing annual growth of 40% in the market [1], optoelectronic devices [23], and soft robotics [24]. Among the devices needed for the development of these fields are batteries for energy storage.

One overlooked aspect of flexible electronic devices is that powering them must also have this bending attribute. Among the many types of energy-storage devices evaluated as candidates to achieve the flexibility needed, metal-air batteries have become very promising due to their high energy density with a relatively simple, safe chemistry. These devices differentiate themselves by having the cathode outside the battery, because they use oxygen from air as agent for electrochemical reactions [2]. The need for flexible batteries and the impact of novel battery materials and architectures is then the motivation of the present project.

Despite the fact that the energy-storage devices market is dominated by lithium-ion batteries, it seems that this technology has reached its maximum development peak, and further improvement could bring only an additional 30% increase in energy density [25]. Thus, metal-air batteries are a promising replacement for Li-ion batteries in applications where high energy density is needed. The main parameters evaluated for efficient batteries are high open-circuit voltage (OCV), operating voltage, energy efficiency, specific capacity, energy density, power density, and cyclic stability [2]. Commercial devices feature different values depending on the type of cell. LiCoO2 / graphite pouch cell values, for example, are reported around 140 mA h g^{-1} and 3.85 V vs. Li/Li^{+} [26]. In this lithium-predominant context, this alkaline metal as anode material for metal-air batteries was evaluated because of his high specific energy of 5928 W h kg^{-1} and high cell voltage of 2.96 V [2]. However, Li-air batteries

had many drawbacks and limitations like cost and scarcity. The trend in lithium prices seems to be stabilized between 4000 and 5000 USD/ton from 2009 to 2015, with a drop in 2011 to 3879 USD/ton [5]. Just to mention a few examples, lithium prices in October, 2017 were more than twice the zinc prices, as well as 9% more than cupper prices [4].

Lithium supply has been an important topic of discussion because of its importance for technological development and the fear caused by its scarcity. There is almost 10 ppm of lithium in the continental crust, while there are some other rare metals which are ten times more easily found [6]. Moreover, the demand of lithium is predicted to rise annually 16% in the following five years, mainly because of the increase in demand of batteries for transportation [27], but without a productive capacity able to sustain this demand growth, despite the possibility of matching the need in terms of extraction of raw material [28], the price of lithium will increase even more.

For the further development of metal-air batteries and their establishment in the industry, the fabrication cost is important; therefore, predictions of lithium costs are not favorable [5]. Moreover, the lack of production capability and scarcity in the Earth's crust [6] have pushed scientists to look into alternative metals for this technology. More specifically, in Peru the extraction of lithium presents many difficulties in the current sociopolitical framework for the exploitation of the huge deposits of lithium that were found in Puno in 2018. Therefore, other materials should be considered and zinc seems promising due to the high specific energy and volumetric energy density is zinc. Moreover, it represents a good opportunity for the development of technology in Peru using proper natural resources, since it is the first exporter of this metal in the region and third in the world. Zinc deposits are estimated to contribute with 60.1 million of fine metric tons of production for 2050 in Peru, which would mean 170 thousands of millions of USD in sales [4]. Therefore, this work will focus on Zn-air batteries. They have a notable performance, but in order to compete with the Li-based batteries, a further development must be done. This type of energy-storage devices has different improvement possibilities in each of their parts, nonetheless, the most critical problem this technology faces is regarding the air electrode design, especially because

of the need of a bifunctional catalyst for ORR and OER [7], reactions that will be explained in following chapters.

In this sense, the present thesis will be focused on the advantages and opportunities regarding the design of air electrodes, making emphasis in the performance of certain materials in order to help the worldwide efforts of scientists in the development of Zn-air batteries technology. Specifically, this thesis tests previous developed synthesis methods of silver nanoparticles as catalysts for Zn-air batteries and will explore the potential of other silver-based nanoparticles. This work is framed in the need for doing research using the metals and minerals abundant in our soil as a demonstration of the possibility to produce high technology in Peru, not only the exportation of metals or mineral concentrates.

General objective

Perform a literature review on the current advances in materials for flexible cathodes for Zn-air batteries to elaborate a research proposal focused on the development of catalysts for ORR and OER reactions in this electrodes.

Specific objectives

- Present a literature review on Zn-air batteries with a focus on their working principle, different Zn-air batteries developed, and the main challenges this technology faces.
- Perform a theoretical evaluation on silver nanoparticles and polyhydroxy fullerenes as materials for air cathodes with a focus on catalysts for OER and ORR.
- Elaborate a research proposal for testing the materials proposed as air cathodes.

1 CHAPTER I
THEORETICAL FRAMEWORK

This chapter presents a literature review on Zn-air batteries and the main challenges these technology presents with a focus on materials for the air cathode. Also, a theoretical analysis on approaches for improving the performance of flexible air cathodes by changing its materials is proposed. Furthermore, it describes the theoretical basis which allows the establishment of a methodology for the experimental analysis of the proposed materials for air cathodes.

In this sense, the structure of this chapter starts with a general description of batteries, with emphasis on metal-air batteries, which is the focus of this work. Afterwards, a general description of silver nanoparticles as catalysts for ORR and OER and its potential in air cathodes is given. Finally, general information about the characterization techniques and electroanalytical methods widely used for the evaluation of cathodes is presented.

1.1 Working principles of batteries

Electrochemical cells are devices which use reduction-oxidation (redox) reactions to generate electricity. Among them, galvanic or voltaic cells produce an electric current with the transfer of electrons from spontaneous reactions [29]. These cells or group of cells are commonly named batteries.

The redox reaction which takes place in the battery involves a reductive agent and an oxidizing agent. These reactants are found in the electrodes of the batteries, more specifically, in the cathode (positive electrode) and anode (negative electrode). For the reaction to continue, a pathway for counter ions formed is needed. This pathway is the electrolyte of the cell [29].

1.1.1 Cell potentials

The spontaneous flow of electrons in an external circuit from the anode to the cathode is caused by the higher potential energy of electrons in the anode. The difference in the energy per electric charge is denominated potential energy and is measured in volts (V). Then, the cell potential will be the difference of the potentials from the electrodes in the cell. Therefore, this cell potential will depend on the redox reactions within its electrodes, the concentrations of the reactants and products, and the temperature at which these reactions take place [30].

In order to standardize these values, the reactions at 25°C with 1M of reactants concentrations are evaluated. Normally, the reactions of materials against all the possible combinations are evaluated against the standard hydrogen electrode (SHE), which has been given an arbitrary value of 0.0 V. In this sense, the reduction reactions of different electrodes against the SHE at standard conditions are evaluated and the cathode-anode cell potential is then made equal to that of the novel electrode. The potential of galvanic cells will always have a positive value of cell potential, whereas in an electrolytic cell the potential is negative. [30].

In order to evaluate the performance of a battery there are several parameters to take into consideration. These are high open-circuit voltage (OCV), operating voltage, energy efficiency, specific capacity, energy density, power density, and cyclic stability [2]. The first one refers to the potential differences between electrodes, adding to the analysis the effects of the liquid-junction potential resulting from the interaction between electrodes and the electrolyte [31]. The subsequent parameters are a normalization of capacity, energy and power using the weight of a battery, thus, allowing a comparison among batteries from different materials and sizes. Finally, cyclic stability refers to the stability a battery has upon many charge and discharge cycles and after how many of them, the battery starts to decay.

1.1.2 Classification of batteries

Batteries are classified in two main groups: primary and secondary. The main difference between them is that the primary batteries can only be used once, which means

that they are nor rechargeable devices, while the secondary batteries are [32]. Other characteristics of these types of cells are described in Table 1.1.

Primary batteries	**Secondary batteries**
Lower cost	Higher cost
It is not rechargeable.	Allows savings because it can be use more than once.
Disposable	Recharge and maintenance needed.
Commercial ones are smaller and lighter.	Research is being done on the improvement of energy density and size of batteries.
Commercial ones present longer life time and capacity.	Research is being done in longer life time and better capacity of secondary batteries.

Table 1.1. Differences between primary and secondary cells
Source: T. Stobe. Classification of Cells and Batteries [33].

Nowadays, the market is dominated by primary batteries. The Battery Association of Japan shows that, from January to September of 2018, 59.32% of the sales from batteries have been from primary batteries, while 40.68% form secondary batteries [34]. However, due to the advantages that secondary batteries represent and the advances in science, the demand on secondary batteries is increasing.

Furthermore, considering the multiple characteristics of batteries and the difference among them, a more specific classification is needed. Amid the many types of batteries seen in the market and on research, there are the ones listed in Table 1.2.

The focus of this work is metal-air batteries; therefore, the next sections will deepen more into their working principle, and the advantages and disadvantages of this type of battery.

Type		Half reactions	Cell voltage [V]	Energy density [MJ/kg]	Comments	Ongoing research
Primary cells	Zn-carbon dry cell	Zn/Zn^{2+} Mn^{3+}/Mn^{4+}	1.5	0.13	Tends to leak out	Recovery of metals
	Alkaline	Zn/Zn^{2+} Mn^{3+}/Mn^{4+}	1.5	0.5	Like Zn-C cells, but with alkaline electrolytes	Recovery of metals
	Metal-air	M/M^{n+} O_2/OH^-	1.0 – 2.4	4.68 – 4.32	Lighter than many batteries	Rechargeable and performance improvement
Secondary cells	Nickel-cadmium	Ni^{2+}/Ni^{3+} Cd/Cd^{2+}	1.2	0.14	Jelly-roll design for reducing size	Increase stability
	Lead-acid	Pb/Pb^{2+} Pb^{2+}/Pb^{4+}	2.2	0.14	Caution with disposal	Increase stability
	Lithium-ion	$LiMO_2/Li_{1-x}MO_2+xLi^+$	3.6	0.46	Most common in the market	Improve performance and reduce costs

Table 1.2. Types of batteries.
Source: Own elaboration based on data from [32], [35], [36].

1.2 Metal-air batteries

Metal-air batteries have the potential of having high specific energy and energy density, therefore, a great scientific effort is being done on its development [36]. Among the metals test for this application, zinc has driven the attention of researchers due to its theoretical capacity, relatively high stability in aqueous and non-aqueous alkaline electrolytes and price. There are many metal-air batteries designs, which are summarized in Figure 1.1.

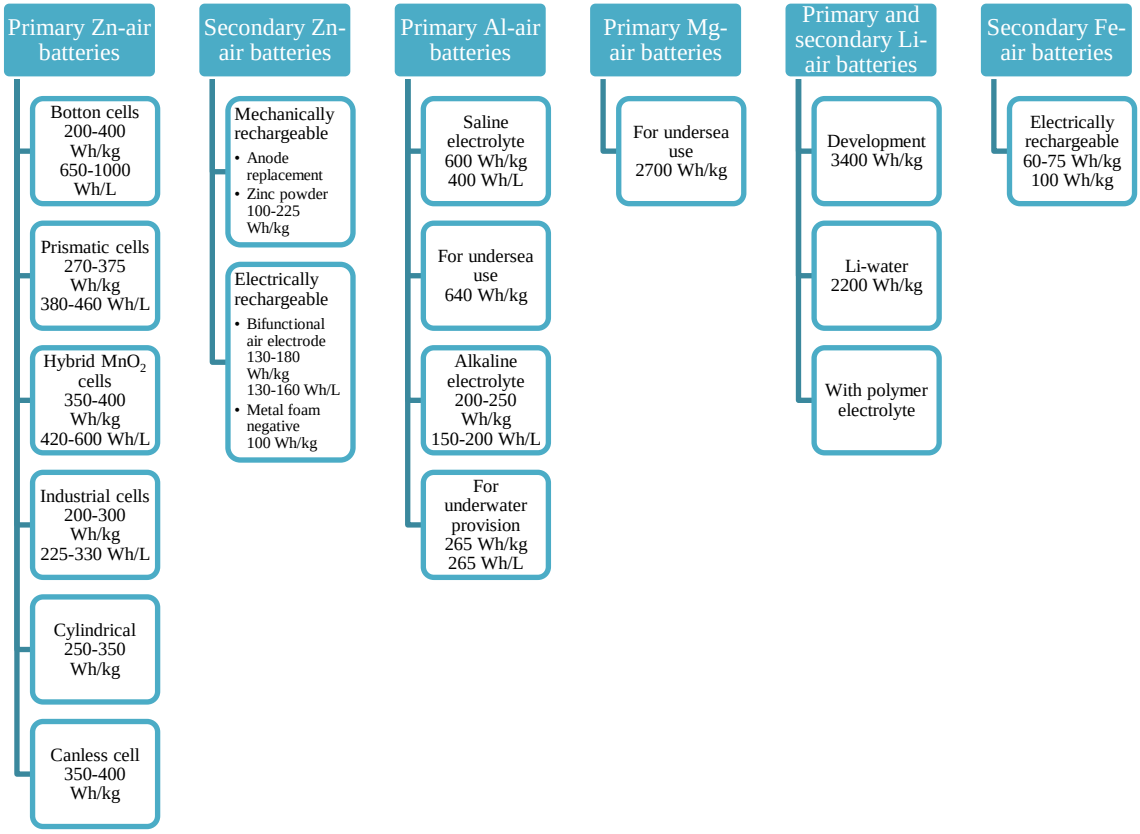

Figure 1.1. Designs for metal-air batteries
Source: T.B. Reddy & D. Linden. Linden's Handbook of Batteries [36].

1.2.1 Working principle

Metal-air batteries are characterized by their high energy density because of their open cell structure, since there is no need to store one of the chemicals (oxygen) inside the battery as the cathode material is the oxygen from the air. Many metals and alloys can act as anode, and depending on them and their reaction mechanisms, the batteries have different architectures and components to satisfy the anode's needs [7].

Many configurations have been explored in metal-air batteries, such as primary, reserve, electrically rechargeable, and mechanically rechargeable ones. The principle of a mechanical recharge is the replacement of the discharged anode, this means that it basically

acts as a primary battery [36]. In order to achieve a conventional electrical recharge, two materials are needed: one to favor ORR and another for OER. However, this would increase the size and weight of the battery. Therefore, a bifunctional air-cathode is preferred [2].

Among the main classification that is used for these energy-storage devices, is the one based on electrolyte type. There are some batteries with aqueous electrolytes, which are not sensitive to moisture; and the ones using electrolytes with aprotic solvents, which are degraded with moisture [7].

1.2.2 Advantages and disadvantages

Even though this battery system has many positive aspects to suit the needs of certain applications, as it was discussed in the INTRODUCTION Chapter, they have also disadvantages. These properties have been summarized in Table 1.3.

Advantages	**Disadvantages**
High energy density	Dependent on environmental conditions
Flat discharge voltage	Limited operating temperature range
Long shelf life	H_2 from anode corrosion
Low cost	Carbonation of alkali electrolyte

Table 1.3. Advantages and disadvantages of metal-air batteries
Source: T.B. Reddy & D. Linden. Linden's Handbook of Batteries [36].

As it was explained previously, the high energy density is due to the lack of storage of the element needed for the reduction, since this is collected from the air and the use of non-bulk metal electrode which is typically lighter than the ones used in the market; as a result, the weight of the battery is significantly reduced. The low cost is also related to the "lack" of an electrode. Usually, electrodes are pieces of metals or alloys in a bulk phase. In the other hand, air-electrodes usually have gas diffusion layer (GDL) with metals or alloys as catalysts impregnated in the form of nanoparticles or particles from smaller size. As a result, the price of the battery is usually determined by the price of the anode [36].

The shelf life is “duration of storage under specified conditions at the end of which a cell or battery still retains the ability to give a specified performance” [36], this is related to the degradation and self-discharge rate of the batteries.

Among the disadvantages of this kind of batteries is the strong dependence on environmental conditions, such as temperature and moisture. Even though many batteries are susceptible to these conditions, in the case of metal-air batteries, its effect are felt in a stronger way due to the need of oxygen from the environmental air for its functioning. This is strongly related to the limited operating temperature range [2].

The H_2 from anode corrosion is favored because many metals reduction potential standards are below the one of hydrogen evolution. The carbonation reaction takes place due to the presence of carbon dioxide in the air, the carbonation of the electrolyte may change the conditions inside the cell [2]. Nowadays, researchers are working in the overcoming of the disadvantages in order to make this technology suitable for certain applications.

As it was explained in the previous section, there are many metals which were analyzed as anodes for metal-air batteries. The first one was lithium, due to the market domain of Li-ion batteries nowadays. However, this component has certain issues such as high cost, low rate of recycling, scarcity, besides the sociopolitical problems related to the beginning of its extraction in the Peruvian context.

There are many other materials that can be used for this application, such as aluminum and magnesium. However, they also present some drawbacks like low coulombic efficiency, irreversibility, and high self-discharge rate. In order to present a better behavior, an alloy between these materials and other metals are done, which increases the cost of the battery. Therefore, and due to the high zinc production in the country, zinc was chosen as anode for the battery in the current work.

1.2.3 Zn-air batteries

Zn-air batteries have four main components: An air electrode, which is mainly composed of a GDL with a suitable catalyst; an alkaline electrolyte; a separator; and, as its name suggests, a zinc anode. During the discharge, zinc suffers a coupling to the air electrode using as bridge an alkaline electrolyte. The electrons that are liberated through this reaction travel to an external load to the air electrode, while zinc cations are produced [2].

Meanwhile, the atmospheric oxygen diffuses through the air electrode and is reduced to hydroxide ions at a three-phase reaction site (molecular oxygen as gas, electrolyte as liquid, and catalyst as a solid). Hydroxide ions react with zinc ions forming zincate ($Zn(OH)_4^{2-}$) ions, which then decompose into insoluble zinc oxide (ZnO). During charging, the oxygen evolves and the zinc deposits in the cathode surface [2]. Equation (1.1) shows the half reaction of the oxygen evolution, Equation (1.2) shows the half reaction of the zinc reduction, and Equation (1.3) presents the overall reaction.

$$O_2 + 2H_2O + 4e^- \Leftrightarrow 4OH^-,\ E = 0.40\ \text{V vs SHE} \tag{1.1}$$

$$Zn + 2OH^- \Leftrightarrow ZnO + H_2O + 2e^-,\ E = 0.8\ \text{V vs SHE} \tag{1.2}$$

$$2Zn + O_2 \Leftrightarrow 2ZnO,\ E = 1.2\ \text{V vs SHE} \tag{1.3}$$

Where

SHE stands for Standard Hydrogen Electrode;

E potential [V]

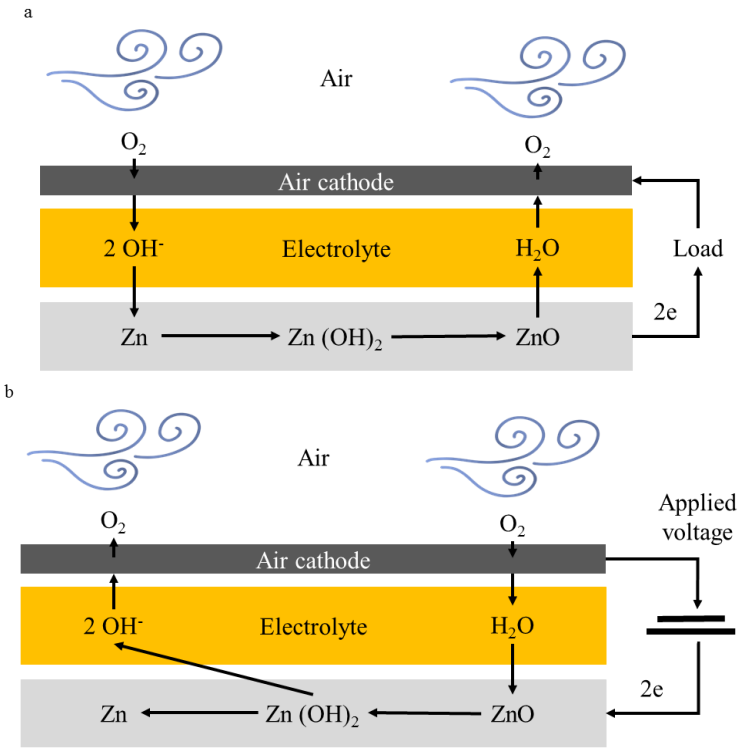

Figure 1.2. Working principle of Zn-air batteries. (a) Charge of the battery. (b) Discharge of the battery.

Source: Own elaboration based on T. B. Reddy & D. Linden. Linden's Handbook of Batteries [36].

Even though all Zn-air batteries work under the same principle, they have different components among their four main parts and different configurations, which have an impact on its performance. These differences are going to be discussed in the following sections.

1.2.3.1 Design and architecture of batteries

There are three main configurations in which Zn-air batteries can be divided, each of them have been built prioritizing different attributes. For example, conventional planar configurations were designed to prioritize high energy density, while Zn-air flow batteries were designed for a longer operational lifetime compared to the conventional planar configurations [2].

a) Conventional planar batteries

Among the planar configurations, the most common one is the button type battery, which is typically build with zinc metal powder as anode and potassium or sodium hydroxide

electrolyte. A cutaway view of this configuration is presented in Figure 1.3, but with silver oxide as cathode instead of a membrane for air collection [36].

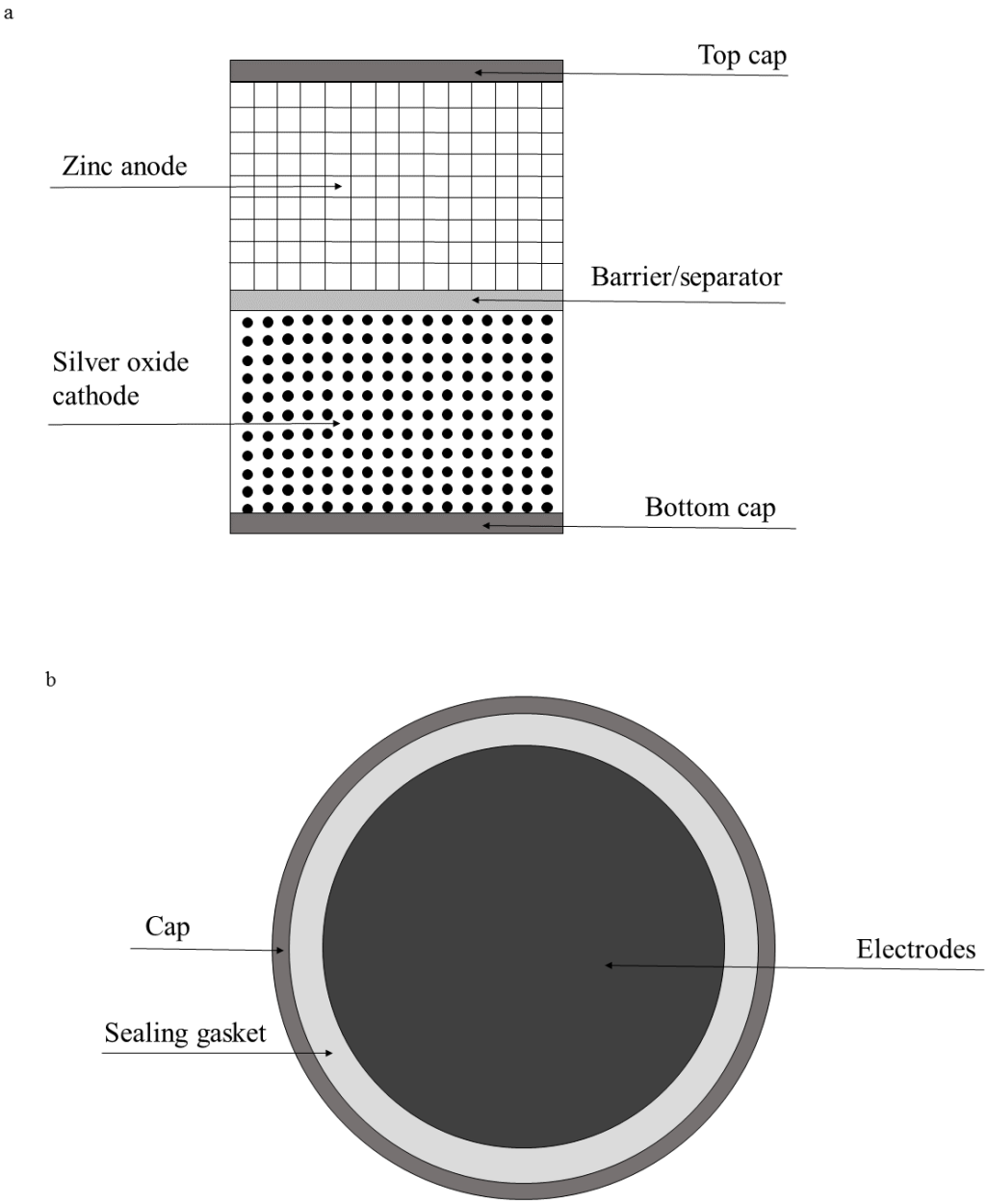

Figure 1.3. Cutaway view of typical Zn/Ag_2O button type battery. (a) Transversal view. (b) Upper view.
Source: Own elaboration based on T. B. Reddy & D. Linden. Linden's Handbook of Batteries [36].

The electrode is put into cups, which acts as current collectors, and separated with a disk of cellophane or grafted polymeric membrane, electrically isolating and ionically conductive layer [2]. This type of configuration is designed to be anode limited, in order to avoid the formation of zinc-iron or zinc-nickel couple that could later origin hydrogen gas formation [36].

Another typical configuration is the prismatic one, which is shown in Figure 1.4. This configuration differs from the button cell in three aspects: Its shape, the conductive current collectors inside the plastic chasing, and external tabs for the electrodes.

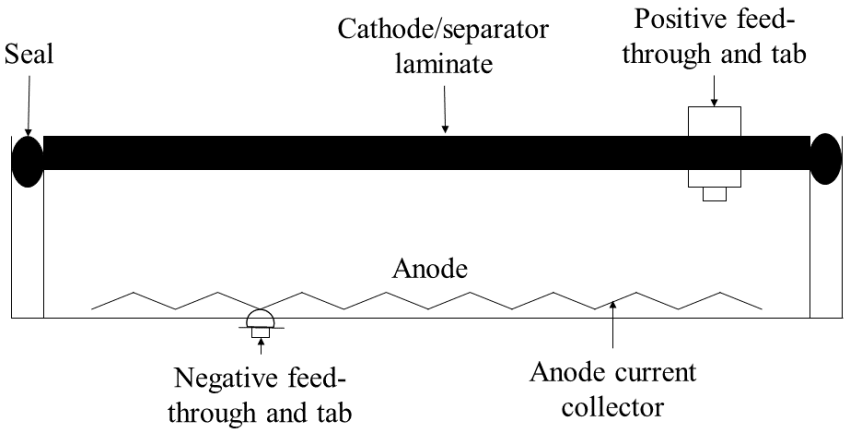

Figure 1.4. Schematics of prismatic primary Zn-air battery
Source: Own elaboration based on R. Putt, *et al.* Advanced Zinc-Air Primary Batteries [37].

The easiest way in which researchers build these cells for tests is by the combination of plastic plates and gaskets fastened together, for a quick assembly and disassembly [2]. Their configuration can be horizontal or vertical [38]–[40]. The advantages of having a horizontal configuration are the better current distribution in the zinc anode and easier oxygen removal from the air electrode. However, it can be seen that it could generate an electrolyte loss due to evaporation [2].

b) Flow batteries

As its name suggests, this configuration has an electrolyte channel through which it circulates in order to increase performance and avoid degradation, as shown in Figure 1.5. This

configuration brings improvements in the functioning of Zn-air batteries, but it also brings complexities. The flow of the electrolyte removes unwanted solids from the air-electrode and improves the current distribution, as a result, there is a decrease in the dendrite formation. However, this configuration increases the complexity in assembly and disassembly and increases the energy density and specific volume[2]. Some companies fabricating these batteries are EOS Energy Storage [41] and Zincnyx Energy Solutions [42].

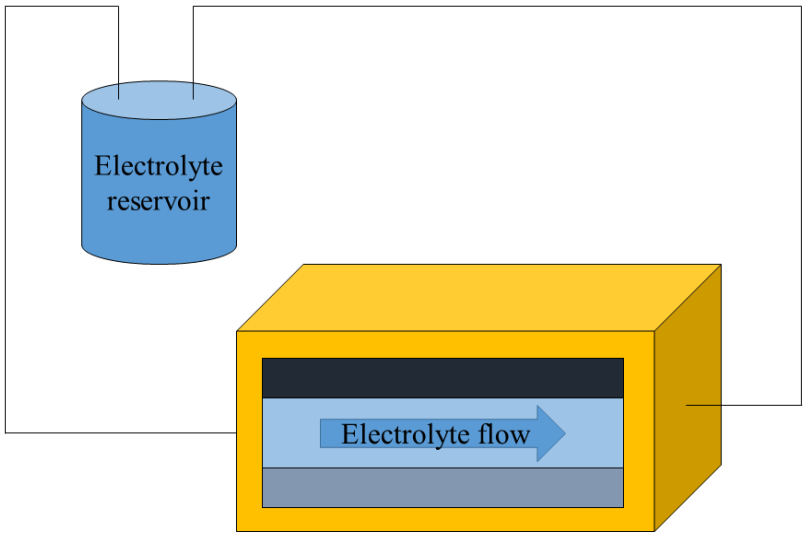

Figure 1.5. Schematic representation of Zn-air flow battery configuration
Source: Based on J. Fu, *et al*. Electrically Rechargeable Zinc-Air Batteries: Progress, Challenges, and Perspectives [2].

c) Flexible batteries

Research on this configuration of batteries is ongoing due to the needs presented in the wearables market, optoelectronic devices and soft robotics, as explained in previous section. Figure 1.6 presents a general schematic of this flexible configuration and Table 1.4 a summary of different types of configuration found in the academia.

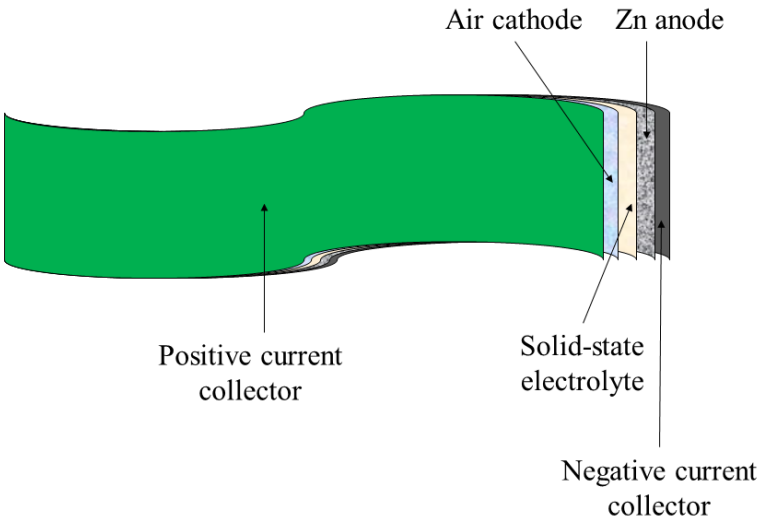

Figure 1.6. General schematic of flexible Zn-air battery
Source: Own elaboration based on J. Fu, *et al*. Electrically Rechargeable Zinc-Air Batteries: Progress, Challenges, and Perspectives [2].

Components	**Design**	**Ref.**
Zn/cellulose film gelled with KOH/Co_3O_4-NCNT	Quasi-solid state	[43]
Zn/KOH with Zn acetate/nanoporous carbon nanofiber films	All-solid state	[44]
Zn/Hydroxide-conductive nanoporus cellulose film/Co_3O_4-NCNT/SS	Hair-like array of air-electrode	[11]
Zn/PPy/MWCNT/BSA	Bio-compatible battery	[45]
Zn/gel polymer electrolyte	All-solid-state cable-type with spiral anode	[46]

Table 1.4. Examples of flexible batteries configurations in academia.
Source: Own elaboration based on data from [43] [44] [11] [45] [46].

d) Multi-cell configuration

This type of configuration is used when higher voltage is needed, which can be accomplished using two different arrangements. In the monopolar arrangement, the zinc electrode is placed between two air electrodes and the cells are repeated and then connected in series through external connections. The bipolar arrangement connects zinc electrodes of adjacent cells through electrically conductive bipolar plate with air-flow channels. In this

arrangement, the air electrode must be electrically conductive, thus, the air-facing part cannot be from poly tetrafluoroethylene (PTFE), which is usually employed because of its hydrophobicity [2].

1.2.3.2 Previous investigations and current challenges

As it was explained before, Zn-air batteries have four different parts and each one of them present opportunities for improvement, which are going to be briefly described in this section.

In the case of the zinc anode, its morphology is the key for a better inter-particle contact and lowering internal electrical resistance [36], many shapes such as powders, spheres, flakes, ribbons, fibers and foam have been studied. Some efforts are been made to increase the anode's surface area without increasing the corrosion, for which many alloys have been studied [47].

J. Fu and coworkers describe four major phenomena which limit its performance, these are summarized in Figure 1.7. One is related to the influence of the shape of the anode on the battery performance. The increase in density of the electrode reduces the capacity. Dendrites are sharp, needle-like metallic lumps that may form during charging due to a gradient in the concentration of $Zn(OH)_4^{2-}$ during reduction. They can fracture and disconnect or break the separator and cause a short-circuit [2]. In order to avoid dendrite growth, charging modes and electrolyte management is suggested; furthermore, the mechanisms of dendrite growth are being studied [48]. Moreover, discharge trapping electrode additives are added in order to hold the $Zn(OH)_4^{2-}$ close to its original position near the zinc anode. Calcium and aluminum are commonly used for this purpose [49], [50] and further research is made on this topic.

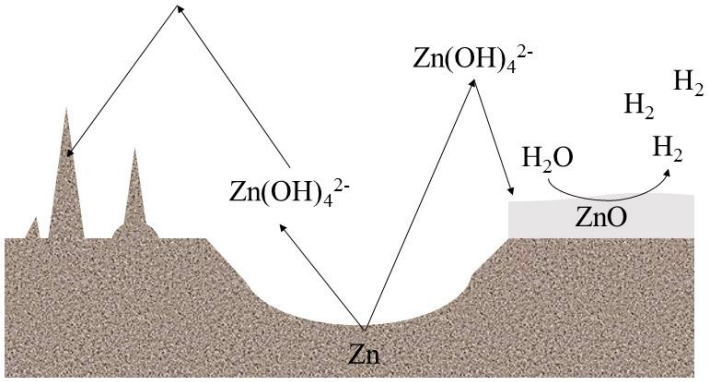

Figure 1.7. Schematic representation of performance-limiting phenomena in Zinc anode. (a) dendrite growth, (b) shape change, (c) passivation, and (d) hydrogen evolution
Source: J. Fu, *et al.* Eectrically Recheargeable Zinc-Air Batteries: Progress, Challenges, and Perspectives [2].

Sometimes, an insulating film is formed on the surface of the zinc anode due to the precipitation of ZnO into de zinc surface caused by the solubility limit of $Zn(OH)_4^{2-}$, thus hindering the migration of ions for the charge and discharge. This phenomenon is called passivation. In order to avoid this, and to lower the zinc anode resistance, scientists are studying the effects of carbon-based additives like carbon black [51]. The last phenomenon was explained before because it is common to many metal-air batteries. H_2 formation is caused because of the difference between the standard reduction potential of Zn/ZnO (-1.26 V SHE) and the hydrogen evolution reaction potential (-0.83 V SHE); therefore, H_2 evolution is thermodynamically favorable [2].

There are two main types of electrolytes, the aqueous and solid-state electrolyte. The most common ones are the aqueous electrolytes, among which stand the hydroxides of potassium, lithium and sodium. Research efforts are driven towards electrolytes with superior ionic conductivity and reducing their vulnerability to carbon dioxide, in order to prevent the formation of carbonates which may block pores from the air electrode. Recently, solid-state electrolytes have drawn the attention of scientists because of the combination of mechanical properties from solids and the ion conductivity of liquids.

One of the challenges when dealing with this type of electrolyte is the improvement of interfacial properties to overcome interfacial resistance to hydroxide ions transporting over

the catalyst surface due to their poor wetting properties [2]. There are two methods for building solid-state electrolytes. The first one is to impregnate basic functional groups into polymer backbones with a single phase. Examples of this are alkaline anion-exchange membranes. The second method consists in the incorporation of alkaline salts into an inter polymer matrix, like gel electrolyte membranes [52].

Due to the nature of rechargeable Zn-air batteries and the air cathode, the focus of the proposal in this thesis is an electrode which must be bifunctional. This means it must be suitable for both ORR and OER. Furthermore, it must be stable and with a wide potential working range. The most common configuration for air cathodes consist of a hydrophobic GDL and a moderately hydrophilic catalyst layer for ORR and OER [7]. According to [2], GDL has four important functions:

i. Provides physical support for the catalyst or catalyst layer.
ii. Promotes a uniformly distributed transportation of O_2 to and from the catalyst.
iii. Prevents aqueous electrolyte from leaking out.
iv. Provides a pathway for current collection.

Therefore, GDL should be thin, conductive, highly porous, and hydrophobic. Scientists are focusing their search for air-electrodes in nonprecious alternatives, in the aim of reducing costs, and carbon-bases materials [53].

Nowadays, there is a need in increasing their stability towards oxidation potential and under alkaline electrolytes. On the other hand, metal based GDL had shown a higher electrical conductivity and better electrochemically oxidative stability [2]. It has been recorded that a uniform distribution of micropores in GDL alleviate the negative influence of the change in porous geometry [54].

Regarding the catalytic activity, the kinetics of ORR and OER stunts the scientists due to the unpredictable reactions. The reduction of oxygen may take two different pathways: four-electron and two-electron mechanisms, which are shown in Equation (1.4) and Equation (1.5) respectively. From both, two-electron mechanism is not preferred due to the poisoning

that the electrolyte of carbon material may cause [2]. On the other hand, the four electron mechanism has a higher energy efficiency due to the higher amount of electrons involved. The latter one is predominant on noble metals [55]. Therefore, using silver supported on carbon as catalyst is a promising arrangement for an air cathode.

$$O_2 + 2H_2O + 4e^- \Leftrightarrow 4OH^- \quad (1.4)$$

$$O_2 + H_2O + 2e^- \Leftrightarrow HO_2^- \, OH^- \quad (1.5)$$

Carbon materials have shown to be good supports which help increasing the number of active sites at the electrode/electrolyte interface, thus, helping in the reaction. Moreover, they show catalytic activity for ORR. However, it has a low OER catalytic activity and has shown to be susceptible to corrosion in this reaction. There are three breakthroughs that have been made from carbon materials which has shown good catalytic activity: Metal-organic framework, hybridizing graphene with CNT and coupling inorganic nanomaterials with functionalized carbons [2].

1.3 Synthesis of silver nanoparticles

There are numerous catalysts which have been used for ORR and OER, among low-cost metals and non-metallic catalysts. Silver nanoparticles stands out for their ORR activity and excellent corrosion resistance in alkaline electrolytes [56], [57]. Therefore, their synthesis have been extensively studied and various techniques have been developed [58].

There are two approaches for growing nanoparticles: bottom-up and top-down. The first one involves the use of a precursor to form metal atoms which nucleate to form particles in the nanoscale size; this includes methods like chemical synthesis, chemical synthesis assisted by radiation, photochemical synthesis, and electrochemical synthesis [59]. The top-down approach, where metal is broken down by shear forces to form nanoparticles, is mainly based on physical growing [60]. From both, a bottom-up approach, chemical reduction, is the most widely used for silver nanoparticles synthesis. For this method, reducing- and stabilizing- agents are needed. Generally, sodium borohydride, sodium citrate, hydrazine and

ascorbic acid are used as the reducing agents and poly(vinyl alcohol), poly (vinylpurrolidone) cetyltrimethylammonium bromide and sodiumdodecyl sulphate are used as stabilizing agents [61]. In this method, the reduction of silver ions take place in controlled conditions to reduce the probability of nucleation. These conditions include:

i) Use of low concentrations of silver ions and reducing agent.
ii) A correct stirring speed, not too slow for a slow dilution of silver solution and not too fast for clashing silver nuclei.
iii) The use of a stabilizing/capping agent to favor repulsion of nanoparticles.

The stability in nanoparticle formation may occur through two types of mechanisms: Steric and electrostatic repulsion. The first mechanism is based on the absorption of polymers and non-ionic surfactants in the phase interphase, where attractive and repulsive forces depend on the thickness of the layer. In the second mechanism, the surface charge of the disperse phase can be enhanced by ionic surfactant addition providing the electrostatic protection of the nanoparticles from adhering between them [62]. In this sense, sodium citrate is an example of electrostatic repulsion mechanisms and polydroxy fullerene (PHF) is an example of the steric repulsion mechanism, as long as it is in a molecular, not ionic, state.

Sodium citrate is used for silver- and gold nanoparticles formation [63]. In this case, the reduction of silver takes place as shown in Equation (1.6), the sodium citrate acts not only as a reducing agent but also as a capping to favor the repulsion of nanoparticles in order to avoid agglomeration [18].

$$12AgNO_{3_{(ac)}} + 14C_6H_5O_7Na_{3_{(ac)}} \rightarrow 12Ag^0_{(s)} + 15C_5H_4O_5Na_{2_{(ac)}} + 9CO + 12NaNO_{3_{(ac)}} + 5H_2O \quad (1.6)$$

The reducing potential of the salt increases with temperature; therefore, relatively high temperatures are preferred. The formation of silver nanoparticles is strongly affected by the concentration of the reducing agent, the pH of the solution, the boiling time and the

stirring speed of the reactants. The correct pH of the solution depends on the reducing agent and the synthesis method, and has a direct effect on the particle's size and form. The use of sodium citrate results in a slower reduction reaction and the particles are angled towards aggregation; notwithstanding, its use is less toxic in comparison to other reducing agents [63].

PHF is a fullerene (C60, an allotrope of carbon) which is terminated with hydroxyl groups after a chemical treatment, which structure is shown in Figure 1.8, and has shown to be promising in many applications in the field of medicine [64]. Functionalized fullerenes have been reported to reduce oxidative stress by scavenging reactive oxygen species and to possess antioxidant properties [65]. It has also been used to accelerate photocatalytic degradation of contaminants [66]. K. Kokubo, *et al*. demonstrated that PHF could be used as unimolecular mimic of oxidized carbon materials used as support for gold nanoparticles [67]. These ligands have an effect on the size of the synthesized nanoparticle and their electronic properties could enhance the catalytic activity of the nanoparticle [68]. M. Islam, *et al.* demonstrated that stabilized gold nanoparticles by fullerenes enhanced the photocatalytic degradation of methyl orange and the catalytic reduction of 4-nitrophenol [69]. For these reasons, it is hypothesized that PHF can be used as reducing agent in the synthesis of silver nanoparticles at the same time it acts as stabilizer and enhance its catalytic activity towards ORR and OER.

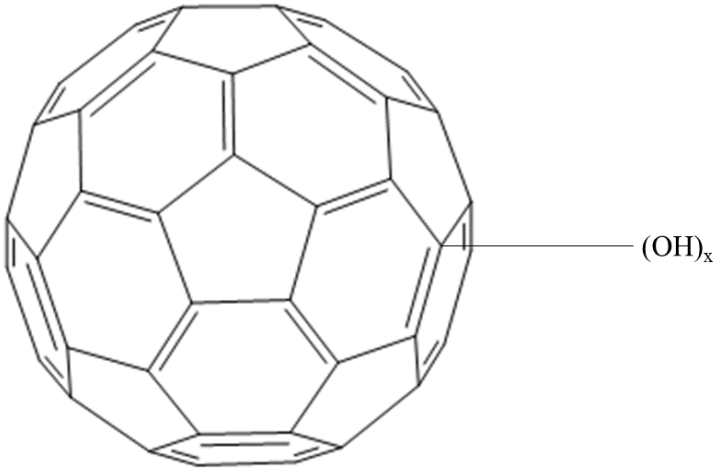

Figure 1.8. Chemical structure of polydroxy fullerene molecule.

1.4 Characterization methods for electrode materials

The focus of the proposed study is the development of materials for the air-cathode; as such, the developed material will need to be characterized in order to make a further analysis for a correlation between them. Thus, in the following sections, the main characterization techniques commonly used are described. While ultraviolet - visible absorption spectroscopy (UV-vis) has been used for the determination of nanoparticles size and the distribution of sizes in solution, before the impregnation, X-ray photoelectron spectroscopy (XPS) is a surface analysis technique used to determine the material's composition.

1.4.1 X-ray photoelectron spectroscopy

XPS is one of the most often applied techniques in the characterization of solid surfaces [70] because it provides information on the composition of the sample, the chemical environment and oxidation states of the different elements. This characterization technique is based on the photoelectric effect by which the energy of a photon is absorbed by an atom and, as a result, an electron is rejected with a specific kinetic energy. This process is described by the Equation (1.7).

$$E_k = h\nu - E_b - \varphi \tag{1.7}$$

Where

E_k the kinetic energy of a photoelectron in eV;

h the Planck's constant 4.14 x 10^{-15} eV s [71];

ν frequency of the incoming radiation in Hz;

E_b binding energy of the photoelectron with respect to the Fermi level of the sample in eV;

φ work function of the spectrometer in eV [72].

Usually, the X-ray sources are Mg Kα and Al Kα, whose energies ($h\nu$) are set to 1 253.6 eV and 1 486.3 eV. Therefore, $h\nu$ in Equation (1.7) is a known, controlled value. The intensity of photoelectrons is measured as a function of their kinetic energy. With this information, the binding energy can be found using Equation (1.7). Usually, the results are plotted in graphs which show the intensity of photoelectrons against E_b [72].

Additional to the peaks obtained due to the photoelectric effect, there are also some peaks observed that are originated by Auger electrons. Even though some peak values from Auger electrons are already reported and well known, one way to differentiate them from those caused by the photoelectric effect, is to perform a measurement in a sample with two different X-ray sources. These electrons have fixed energy, this means they are independent from the X-ray source; therefore, the Auger peaks will appear shifted on the binding energy scale [72].

1.4.2 Ultraviolet and visible absorption spectrometry

The absorption of light from different species is unique, therefore, it can be used for qualitative and quantitative analysis of organic and inorganic compounds [73], as well as nanoparticles. In this test, samples are illuminated with electromagnetic waves from different wavelengths in the range of visible and ultraviolet spectrum and the transmitted rays are recorded to form a spectrum. Usually, what is plotted in this analysis is the absorbance (A_b), which is defined as the negative logarithm of the transmittance (T_r). Moreover, this technique gives information about the concentration of a sample in accordance of the Lambert-Beer law, which is showed in Equation (1.8):

$$c = \frac{A_b}{\varepsilon d} \tag{1.8}$$

Where

c concentration in a sample given in mol L^{-1};

ε extinction coefficient given in L cm^{-1} mol^{-1}; and

d path length given in cm [74].

Metallic bonds formed on the surface of these materials are compared with plasma because of the free electrons in the conductive band surrounding the nuclei. The collective excitation of the electrons near the surface of the nanoparticles is known as surface plasmon resonance (SPR). These electrons are limited to specific vibrational modes by the size and form of the particle. This is the reason of the colors they display when formed, different from the bulk form of the metal. This means that each metallic nanoparticle presents a unique optical absorption spectrum in the UV-vis range of light [75].

In this sense, a solution containing nanoparticles displays a unique UV-vis spectrum in which the peak position is related to the particle size, the full width at half maximum is related to the dispersion of this particle size and the absorption peak indicates the concentration of nanoparticles of this specific size [18].

1.5 Electroanalytical methods

Electroanalytical methods are the ones used to examine an analyte based on oxidation-reduction reactions, and are commonly used to analyze the behavior of an electrode and test its performance. These methods can be classified into two groups: interfacial methods and solution methods. The first main group focuses on the phenomena that take place between the electrodes and the solution next to it; while the second group isolates the solution from the interfacial effects. The interfacial methods group can be further divided into static and dynamic methods. The main difference between these two subgroups is the possibility of controlling the current in the cell, since the static methods do not use a current for the test, while the dynamic methods do [73]. A summary of the methods presented in this section is found in Table 1.5.

Test	Parameters studied	Variables	Nature
Open circuit potential	Potential [V]	Electrodes and electrolytes	Static
Cyclic voltammetry	Current [A] Redox process	Applied voltage [V]	Dynamic
Galvanostatic charge-discharge	Capacity [Ah]	Current density [$mA\ cm^{-2}$]	Dynamic

Table 1.5. Summary of electroanalytical tests.
Source: Own elaboration based on [2], [36], [73], [76]–[80].

1.5.1 Open circuit potential

The open circuit potential (OCP) is the electrode potential at which there is no current flow [81]. The measured OCP is the sum of the potential differences in the interfaces of a cell [82] at a non-equilibrium state [31]. This value is measured over time to determine the stability of the electrode potential over time. This value is firstly used to determine the start potential of further electroanalytical tests, like cyclic voltammetry. Moreover, its value gives a first sight of the voltage of a battery, since the other electrode has a known potential [31].

1.5.2 Cyclic voltammetry

Voltammetry is a group of electroanalytical methods in which the current is measured as a function of an applied voltage under conditions that promote the polarization of the analyte, for which the electrodes are as small as possible (in the order of a few millimeters) [73]. Polarization is one of the two phenomena that increase the potentials from the Nernst Equation when exposed to a current, as it can be seen in Equation (1.9).

$$E = E^0 - \frac{RT}{nF} \ln C \tag{1.9}$$

Where

E potential difference in V;

E^0 potential difference under standard conditions in V;

R universal gas constant 8.316 J mol^{-1} K^{-1};

T temperature in K;

n number of mol of electrons transferred in the reaction;

F Faraday constant which is equal to 96 485 C mol^{-1}

C reaction quotient [76].

The type of cell for the voltammetry test varies depending on the analyte and the type of voltammetry. The most common one is the three-electrode configuration, which has four main components that are shown in Figure 1.9:

a) Electrolyte solution: Consists of the analyte and a supporting electrolyte dissolved in a solvent (typically water).
b) Working electrode: Is the electrode to be tested (made of the material under investigation). Its potential is varied respect to the reference electrode.
c) Reference electrode: Electrode with a known, constant potential throughout the whole test. As explain before, the potential of an electrode must be measured against another electrode, being the standard hydrogen electrode the most common one. However, during the measurements, there are many electrodes that may be used.
d) Counter electrode: It is often a coil of platinum wire and is the one which closes de circuit with the working electrode.

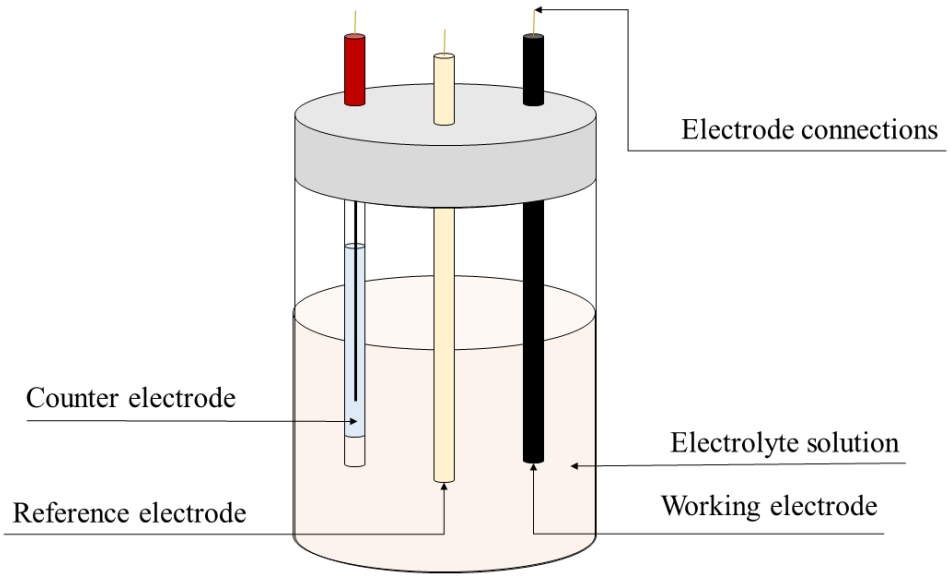

Figure 1.9. Schematic representation of an electrochemical cell for voltammetry
Source: Own elaboration based on N. N. Elgrishi, *et al*, A Practical Beginner's Guide to Cyclic Voltammetry [77].

The input signal for the voltage DC can be either of the four types: linear scan, differential pulse, square wave, or cyclic voltammetry. Only cyclic voltammetry, which pulse is shown in Figure 1.10, is going to be explained in this section, as it is part of the proposed methodology.

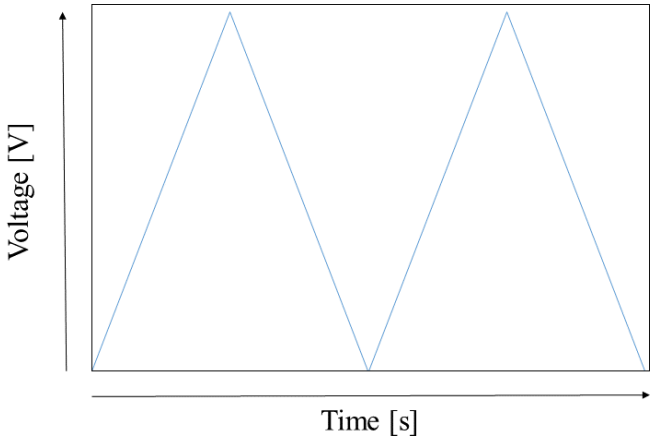

Figure 1.10. Voltage vs. Time excitation signals in cyclic voltammetry
Source: Own elaboration based on D.A. Skoog, *et al*. Fundamentals of Analytical Chemistry [73].

As its own name suggests and can be seen in the excitation signal from Figure 1.11, the cyclic voltammetry allows the study of reduction and oxidation processes, and electron transfer-initiated reactions. Usually, cyclic voltammogram shows an arrow for the reduction process, the US convention shows the potentials in a decreasing way, while the IUPAC convention shows them in an increasing way [77].

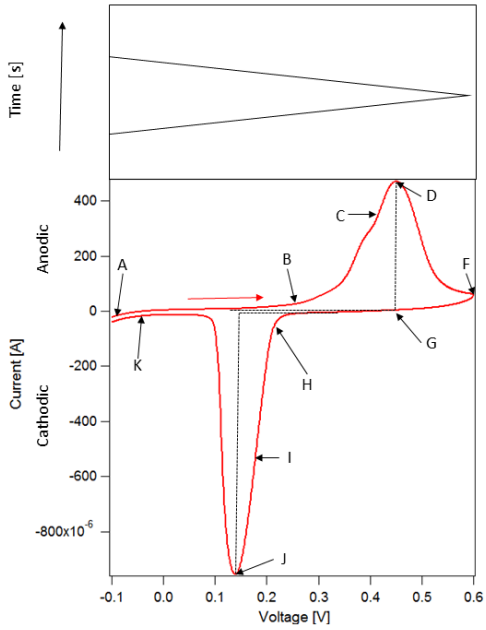

Figure 1.11. (a) Potential vs. time waveform. (b) Cyclic voltammogram
Source: Own elaboration based on [73].

Figure 1.11 shows a cyclic voltammogram, which is taken as a reference to explain the analysis of a voltammogram. The Figure 1.11(a) shows the potential input and Figure 1.11(b) the system response. At the beginning, a small cathodic current is seen, but it quickly reaches zero for several potentials until it becomes more positive and an anodic current starts to develop in point B. At D, the maximum current is achieved by combining two components. One is determined by the Nernst equation as the current required to achieve the equilibrium concentration. Other is determined by the delivery of the normal diffusion-controlled current [73].

The current starts to decay between D and F because the diffusion layer grows further from the electrode. As can be seen in Figure 1.11 (a) , the potential starts to increase, but the current stays anodic until it reaches zero and a reduction of the compounds that has been oxidized previously takes place [73]. On points C and I, the concentration of the ions are equal on the surface of the electrode, this means $E = E_{1/2}$. This value is used to solve the Nernst equation for specific reversible reactions. The difference between the anodic and

cathodic peak is called peak-to-peak separation when the reaction is chemically and electrochemically reversible [77].

One important parameter of this test is the scan rate, which is the velocity at which the potential is scanned, because faster rates may decrease the size of the diffusion layer and increase the current peaks. The Randles-Sevcik equation, shown in Equation (1.10), describes the increase in current peak and indicates if the analyte is freely diffusing in a solution.

$$i_p = 2.686\ 10^5 n^{3/2} A C^0 D_0^{1/2} v^{1/2} \quad (1.10)$$

Where

i_p peak current in A;

v scan rate in V s^{-1};

A electrode surface area in cm^2;

D_0 diffusion coefficient of the oxidized analyte in $cm^2\ s^{-1}$

C^0 bulk analyte concentration mol cm^{-3} [73].

In this test, the catalytic activity of a material can be determined by analyzing the onset potential of the peaks of interest and the amount of current this peaks represent. Each peak corresponds to a reduction or oxidation reaction, depending on the polarity of the current (cathodic or anodic). The onset potential is related to the amount of energy required for a reaction to take place, the closer it is to zero, the less energy is required for the reaction to take place. The amount of current in a peak, is related to the amount of reacting compounds, therefore, a higher peak indicates a higher amount of reacted compounds. In this sense, better catalysts show onset potentials closest to zero and large amount of current in the peaks of the reactions they are enhancing [83].

1.5.3 Galvanostatic charge-discharge test

As its name suggests, this test charges a battery and discharge it at specific current densities rates, usually measured in mA cm^{-2} [17]. This test shows at which current there is

a saturation, the stability of the electrode upon several cycles, as well as the capacitive and faradaic behavior of the electrode and its capacitance [84].

When the voltage is plotted against the capacitance, the slope of the graph indicates the capacitive or faradaic effect. In this sense, a change in the slope as shown in green in Figure 1.12, is attributed to a faradaic effect. On the other hand, a constant and smooth slope is attributed to a capacitive effect, as shown in red [84]. The faradaic effect is common to batteries, while the capacitive effect, as its name suggest, is common to capacitors. The Figure only shows one cycle for demonstrative purposes.

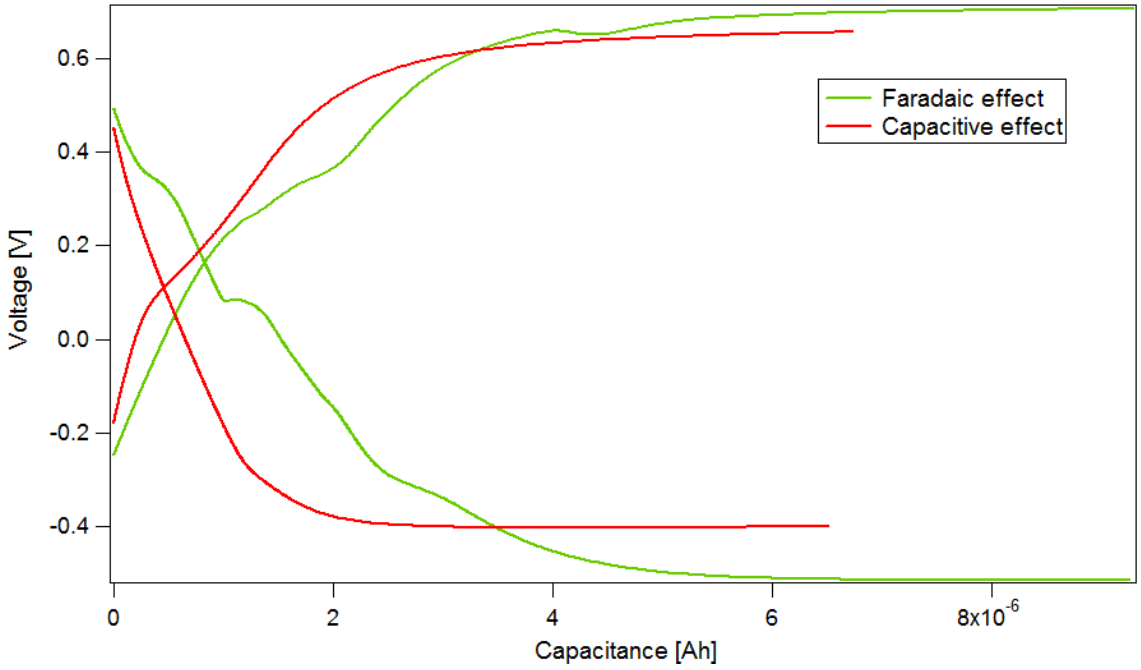

Figure 1.12. Voltage vs. capacitance graph example.
Source: Own elaboration

A plot voltage vs. time gives other type of information. An example is shown in Figure 1.13, where the graph in blue shows a higher current density than the graph in red. The stability of the electrode upon many cycles can be evaluated, with a drop on the voltage over time being characteristic of an unstable electrode. The stability of the electrode is a desirable characteristic, because it means a longer life time. In the other hand, the end of the

charging gives information about the saturation achieved in that specific current density. If it turns flat, like the graph shown in blue, then there is a saturation; conversely, if it has a slope as shown in red, then the saturation is not reached at that specific current density. In the discharge part of the curve, the resistance to discharge is evaluated. If there is a smooth slope, then there is a resistance to discharge, but a sharp slope as shown below, indicates a rapid discharge, which is a desirable characteristic for an electrode. The change in the slope explained in Figure 1.12, can also be seen in this type of graphs. In this case, no change in slope is shown in the charge nor discharge, therefore, a capacitive effect is attributed [84].

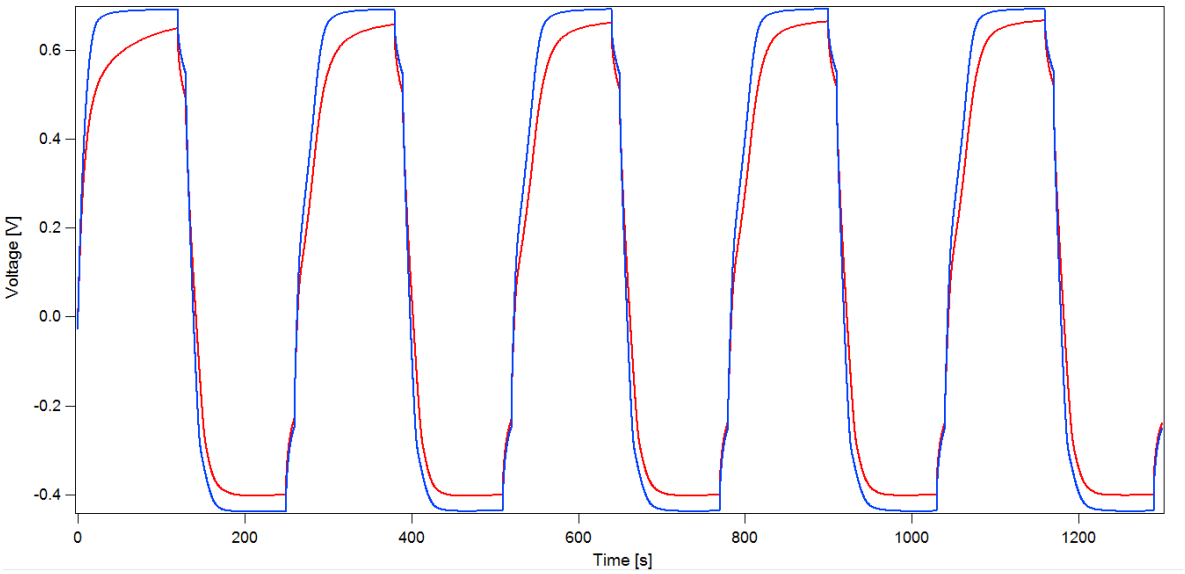

Figure 1.13. Voltage vs. time graph example.
Source: Own elaboration.

As can be seen, this test gives important information about the electrode. It determines which electrode acts as a battery electrode, and provides information about stability and resistance to discharge, informing therefore how efficient is a proposed electrode for a Zn-air battery.

2 CHAPTER II
METHODOLOGY

Based on the information presented in the previous chapter, new materials for air cathodes for Zn-air batteries will be proposed, as well as a methodology for testing its performance. These materials are silver nanoparticles, impregnated over carbon nanotube (CNT) buckypaper (20 gsm C-grade CNT Bucjypaper 12'' x 12'', NanoTechLabs, Inc., Yadkinville, NC, USA) through the ink evaporation method. The synthesis of silver nanoparticles employs sodium citrate as reducing agent and is based on the Frens method for synthesis of gold nanoparticles [19]. Moreover, another synthesis method using polyhydroxy fullerenes (PHF) as reducing agent is proposed, as reported in literature, it acts stabilizer and it is hypothesized to enhance the catalytic activity of the silver nanoparticles towards ORR and OER. The characterization methods considered by the author for silver nanoparticles are UV-vis and XPS, essential for the analysis and a comparison among them and the ones previously developed by the group.

After the synthesis, these materials must be impregnated onto the carbon buckypaper, which works as current collector in the Zn-air battery. The electrode is characterized by OCP, CV and galvanostatic charge-discharge test in neutral and alkaline media. The capacity, catalytic activity and stability of the different proposed electrodes must be evaluated for comparison and the establishment of the most suitable cathode for the battery. The data analysis is key for coming to conclusions, therefore, the use of a suitable software like IgorPro (WaveMetrics, OR, USA) is necessary. This methodology is summarized in and explained in detail in Figure 2.1 the following sections.

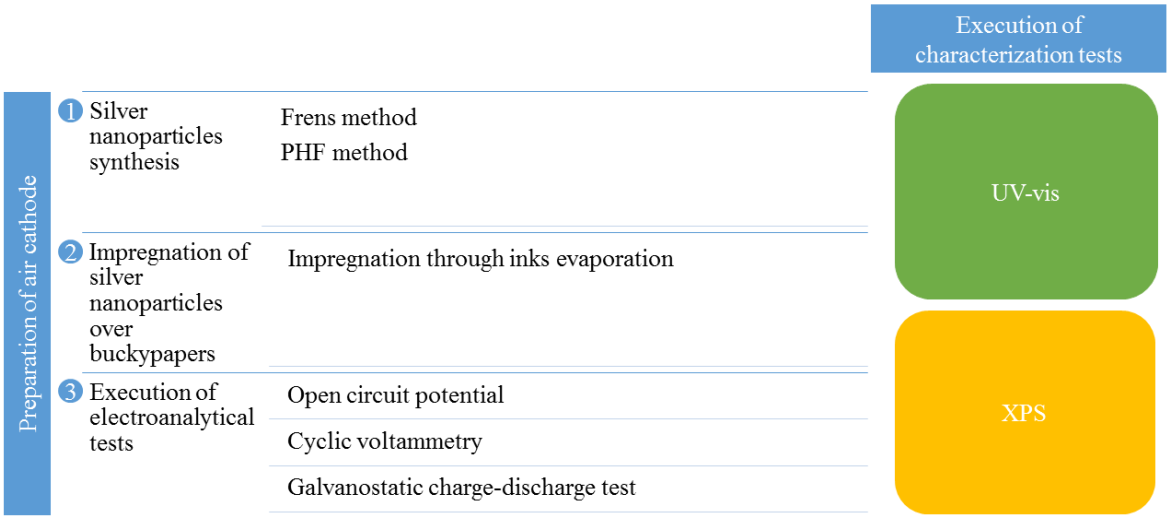

Figure 2.1. Methodology flow diagram.
Source: Own elaboration.

2.1 Preparation of the air cathode

The preparation of the air cathode is done under atmospheric conditions at UTEC facilities. The preparation process itself consists of two steps and a final characterization of the electrode. The two steps are: the synthesis of silver nanoparticles and their impregnation over CNT buckypapers. The characterization of the electrode is done using UV-vis and XPS, and its performance as air cathode is tested using three electroanalytical techniques: open circuit voltage, cyclic voltammetry and galvanostatic charge-discharge test. The detailed step-by-step procedure is going to be explained in the following subsections.

2.1.1 Silver nanoparticles synthesis

2.1.1.1 Frens method

This procedure was presented by M. Gakiya Teruya, L. Palomino Marcelo and J.C. Rodriguez Reyes [19] and adapted for the following work at UTEC laboratories. This procedure uses sodium citrate as reducing agent for the silver nanoparticles formation. As explain in the previous section, an increase in temperature increases the reducing potential of the salt; therefore, the boiling point is reached in this method. On the other hand, in order

to propitiate the fast formation of nuclei and the subsequent slow growth sodium citrate is injected in a short time. This procedure is detailed in the following lines.

A solution of 50 mL of $AgNO_3$ (99.8%, J.A. Elmer, Lima, Peru) in distillated water at 1 mM is placed in an Erlenmeyer flask with a magnetic pill and totally covered with aluminum foil, in order to avoid exposure to light (as showed in Figure 2.3). The solution is heated until boiling point (100°C) and then a 500 µL solution of sodium citrate (at 99.9%, developed by Movilab, Lima, Peru) in distillated water at 0.189 M is added at once using a micropipette. The final solution is stirred for 20 minutes, obtaining a brownish color. Then, this solution is microcentrifugated (with an Eppendorf® Centrifuge 5415 C). This procedure is shown in Figure 2.2.

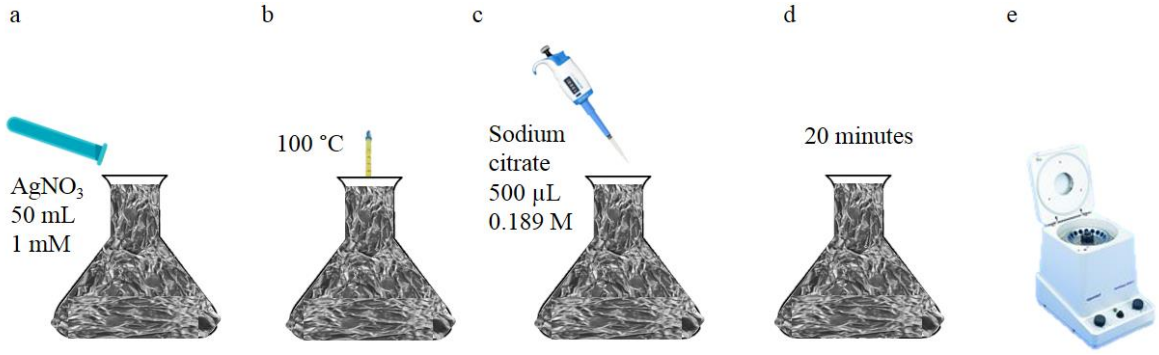

Figure 2.2. Schematic of the Frens method for silver nanoparticles synthesis. (a) Place of 50 mL of silver nitrate in Erlenmeyer flask covered with aluminum foil. (b) Heat the solution until boiling point. (c) Add 500 µL of sodium citrate. (d) Stir for 20 minutes. (e) Microcentrifugate to obtain the silver nanoparticles.
Source: Own elaboration.

Figure 2.3. Erlenmeyer flask with a magnetic pill totally covered with aluminum foil being heated. Source: Own elaboration.

2.1.1.2 Method using PHF as reducing agent

The following procedure was developed by Juan Carlos Rodriguez-Reyes Research Group in collaboration with Cleveland Clinic and adapted for the following work at UTEC laboratories. PHF is used in the silver nanoparticle synthesis as surfactant to enhance the catalytic activity of this catalyst.

For the tests, 5 µL of a solution of $AgNO_3$ (99.8%, J.A. Elmer, Lima, Peru) at 1 M in distillated water, 500 µL of a solution of PHF at 1mg mL^{-1} in distillated water, and 495 µL of distillated water is added to a vial covered with aluminum foil to avoid exposure to light. Then, a shaker (Fisher VM-300) is used for stirring for 4 hours for a later centrifugation at 5712 relative centrifugal force (RCF) for 30 minutes at 25°C. After that, the supernatant is discarded and the pellet is resuspended in distillated water to achieve 1 mL.

2.1.2 Impregnation of silver nanoparticles over buckypapers through inks evaporation method

The inks evaporation impregnation method is used to deposit the silver nanoparticles and PHF over the CNT buckypapers. This method involved the formation of an ink of distillated water and isopropanol (IPA) with the silver nanoparticles and PHF for a further evaporation. The procedure is described in this section. The general schematic is presented in Figure 2.4.

In the case of the impregnation of electrodes with only silver nanopaticles, a resuspension of silver nanoparticles in 800 µL of distillated water and 200 µL of IPA (2-Propanol, developed by J.T. Baker, TM, Madrid, Spain) at 66mM of concentration was made. After that, the solution was sonicated using an DR-S20 Ultrasonic Cleaner 3L (Shenzhen Derui Ultrasonic Equipment Co., Shenzhen, China) for 30 minutes at 25°C. Then, 10 µL of the solution was added to the buckypaper. When the drop was beginning to evaporate, other 10 µL were added until 20 µL were deposited. After the 20 µL solution was deposited, the buckypaper was left under the infrared light for 15 minutes to favor the evaporation of the solvent. This is shown in Figure 2.5.

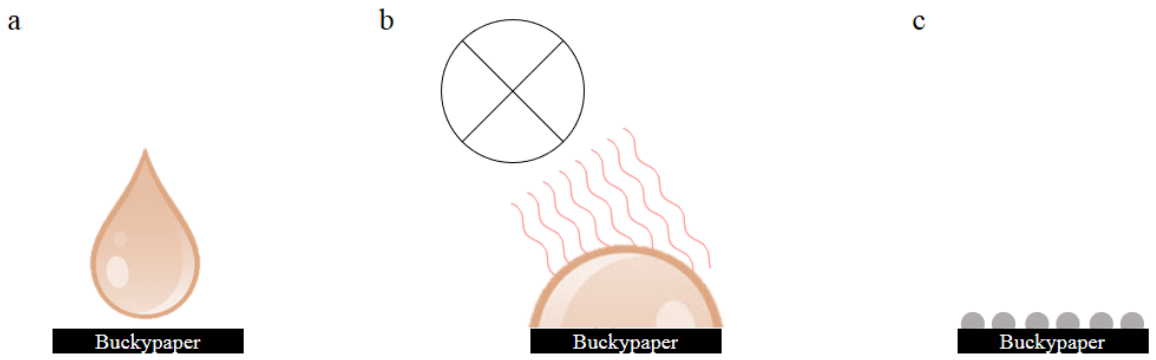

Figure 2.4. Schematic of silver nanoparticles impregnation through inks evaporation. (a) Deposition of colloids over the buckypaper. (b) Irradiation of light over the drop to dry the water and IPA. (c) Schematic of resultant electrode.
Source: Own elaboration.

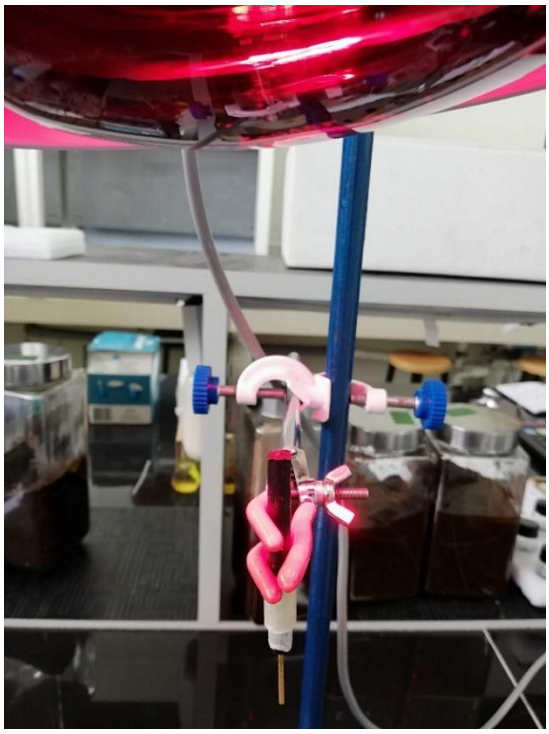

Figure 2.5. Silver nanoparticles ink drying by IR light over buckypaper pasted over carbon vitro work electrode
Source: Own elaboration

In the case of the impregnation of electrodes with silver nanoparticles synthesized with PHF as reducing agent, a solution of the colloid is done in 200 µL of DI and 50 µL of IPA. Each of these is stirred using he vortex. Then, 10 µL of the solution is added to the CNT buckypaper and irradiated with IR light, followed by another 10 µL until the 250 µL is impregnated.

2.1.3 Execution of electroanalytical tests

The electroanalytical procedures are based on the procedures of the Research Group of Applied Electrochemistry at UNI, having in consideration the equipment available in their laboratories.

2.1.3.1 Open circuit potential

This is the first test performed to every electrode tested, to evaluate its potential and stability over time. It is especially important to define the starting voltage value for the CV test. The equipment used for this test is ZIVE SP2 potentiostat (WonATech Co., Ltd., Korea). This test is done using an amplitude of 5 mV, a start frequency of 10^{-6} Hz, a medium frequency of10^{-5} Hz and a final frequency of 10^{-3} Hz, the sample density is 50 point per decade with current range of 20 mA for 120 seconds.

2.1.3.2 Cyclic voltammetry

All the experiments will be done in a three electrode configuration and two electrolytes will be used for neutral and alkaline medium. In the case of the neutral medium, the electrodes used are silver/silver chloride at 3 M as reference electrode, platinum electrode as counter electrode, and carbon vitro as work electrode. For the alkaline medium, the reference electrode was a mercury/mercury oxide electrode (E = 0.165 V vs. SHE) and the CNT Buckypaper acted as working electrode without support. All the electrodes were cleaned with ultrapure water before using them. The set-up used is shown in Figure 2.6**.**

Figure 2.6. Set-up for the cyclic voltammetry.
Source: Own elaboration

The tests in neutral medium uses sodium chloride (EMSURE ACS, ISO, Reag. PhEur) at 1M in ultrapure water as electrolyte and is performed as follows. The CNT buckypaper is put over the work electrode using a Nafion perfluorinated ion-exchange resin (developed by Sigma Aldrich, Darmstadt, Germany). To do it, 1 cm x 1 cm of buckypaper was cut, 10 µL of Nafion was put over the work electrode, and then the buckypaper over the Nafion. Finally, infrared light (IR) is used to dry the sample as shown in Figure 2.5.

Before each test, a cleaning of the electrode is done, followed by a blank experiment using carbon vitro cathode. The cleaning is done as follows: slowly and in an 8-form, the electrode is sanded for 60 times. Then, the tip is cleaned using an ultrasonic bath for 15 minutes in distillated water and washed with ultrapure water (PURELAB Classic, ELGA LabWater, High Wycombe, UK). After that, an electrochemical cleaning using DY2100 Series Mini Potentiostat (Digi-Ivy, Inc., Austin, TX, USA), with a condition time of 180 seconds, a potential during condition time of -0.2V and a quiet time of 5 seconds is done. The general settings for the electrochemical cleaning are shown in Figure 2.7.

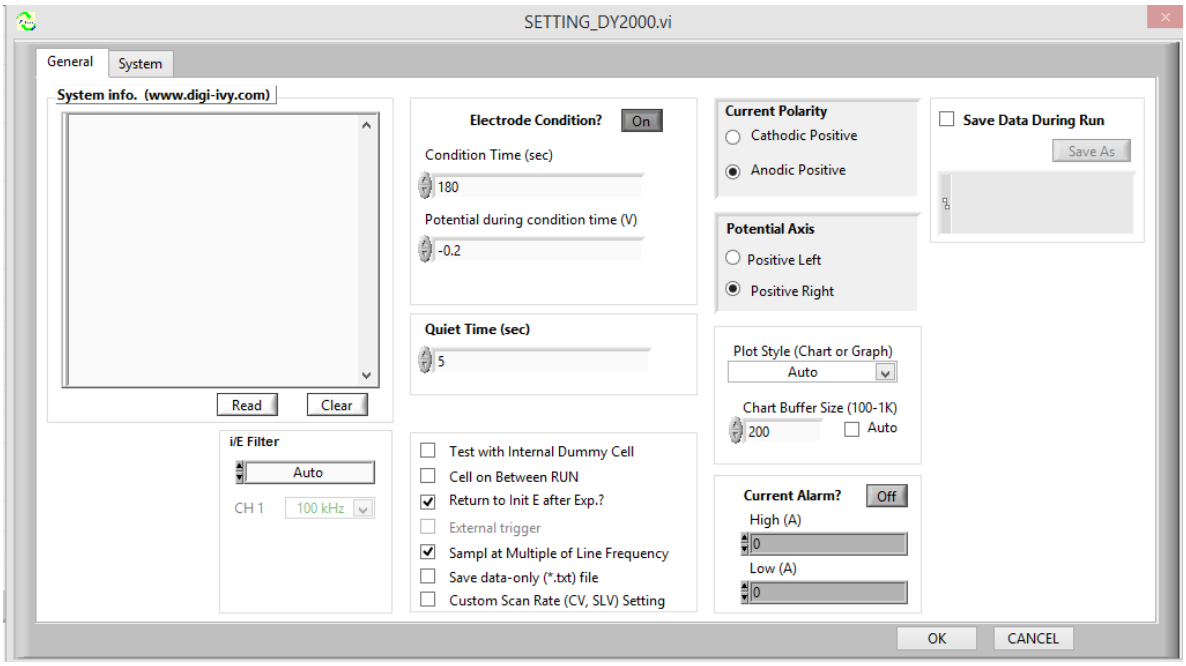

Figure 2.7. Settings for an electrochemical cleaning.
Source: Own elaboration.

The general settings for the cyclic voltammetry in neutral media are an anodic current positive, a quiet time of 5 seconds, a window from -1.2 V to 1.2 V at a scan rate of 0.05 V s^{-1} with a sensitivity of 1 x 10^{-3} for 5 cycles. These settings are shown in Figure 2.8. For the analysis of the data, the average of all the cycles done is used, excluding the first one.

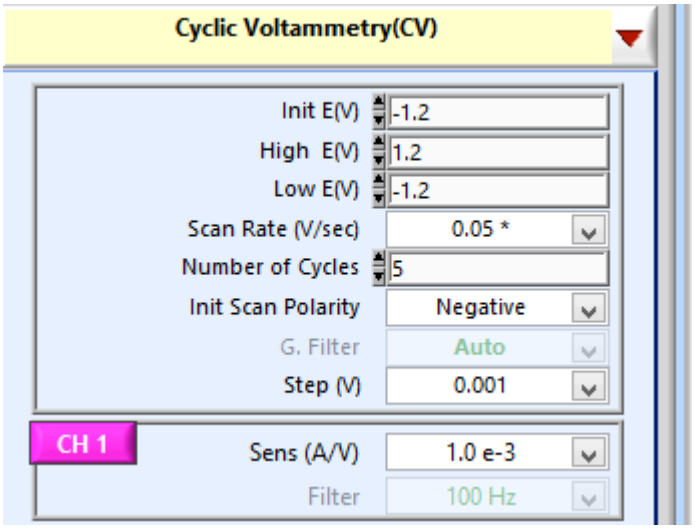

Figure 2.8. General settings for a cyclic voltammetry in neutral medium.
Source: Own elaboration.

The tests in alkaline medium use potassium hydroxide at 0.1 M as electrolyte and no work electrode; instead, the CNT buckypaper (0.5cm x 6cm approximately) with and without silver nanoparticles is connected directly through a female pin terminal (16-14 AWG). The CNT buckypaper is hydrophobic, therefore, it must be wet with Nafion perfluorinated ion-exchange resin before each test for it to be immerse in the electrolyte. At the beginning bubbles are formed around the CNT buckypaper, but after 10 to 15 minutes, the bubbles disappeared and the measurements may start. For the calculations of current density, the only area considered is the one being immersed in the electrolyte. The equipment used for this test was ZIVE SP2 potentiostat (WonATech Co., Ltd., Korea).

The general settings for the cyclic voltammetry in alkaline medium are a quiet time of 5 seconds, a scan rate of 0.02 V s^{-1} with a sensitivity of 1 x 10^{-3} for 3 cycles, the initial potential must be determined using the OCP test and, due to the small differences among the carbon electrodes, all tests started at -0.1V in the first run. According to the IUPAC convention, the anodic current is represented as positive. A wide potential window is use to analyze the reactions occurring in the test, which goes from -0.5 V to 1 V. In addition, shorter windows having in consideration the resulting peaks are taken to confirm the reactions occurring in the process. According to literature, these will be from -0.2 V to 0.6 V and from 0.2 V to 1 V. The results show the average of the cycles excluding the first one, except otherwise is specified. The graphs show current and not current density because the area of impregnation was constant in the samples.

2.1.3.3 Galvanostatic charge-discharge test

In order to evaluate the durability and stability of the cathodes throughout different cycles, galvanostatic charge-discharge test is done. The set-up used was the same as in CV tests, using a three electrode configuration (silver/silver chloride at 3M as reference electrode and platinum as counter electrode) with sodium chloride at 0.1M as electrolyte and ZIVE SP2 potentiostat (WonATech Co., Ltd., Korea) as equipment. The general settings for this test were a charging and discharging time of 120 seconds and 10 seconds from rest time for 5 cycles, a current range of 20 mA and a data acquisition rate of 1mV and 1mA. 0.16 mA,

0.2 mA, 0.24 mA, and 0.28 mA were applied to the electrode. After each test, the immersed area of the electrode in the electrolyte was measured to determine the current density.

2.2 Execution of characterization tests

The equipment of each characterization technique is described in the following sections, as well as the way in which these techniques are used in the analysis of results.

2.2.1 Ultraviolet and visible spectroscopy

The equipments used for this analysis are a NanoDrop® ND-1000, Thermo Fisher Scientific INC (Waltham, MA, USA) spectrophotometer, with a flash-lamp from xenon as light-source with a charge device attached for the refracted beam analysis For using the NanoDrop and analyzing the silver nanoparticles synthesized using the Frens method, the nanoparticles are resuspended in distillated water at 33 mM and 66 mM and for each measurement, 2 µL of sample is used. In the case of the silver nanoparticles synthesized using PHF as reducing agent, the resuspension is done for 5 mM of concentration.

After each synthesis of silver nanoparticles, the NanoDrop® ND-1000 is used for UV-vis characterization. This test determined the size, size dispersion and concentration as explained in previous sections. This is shown in Figure 2.9.

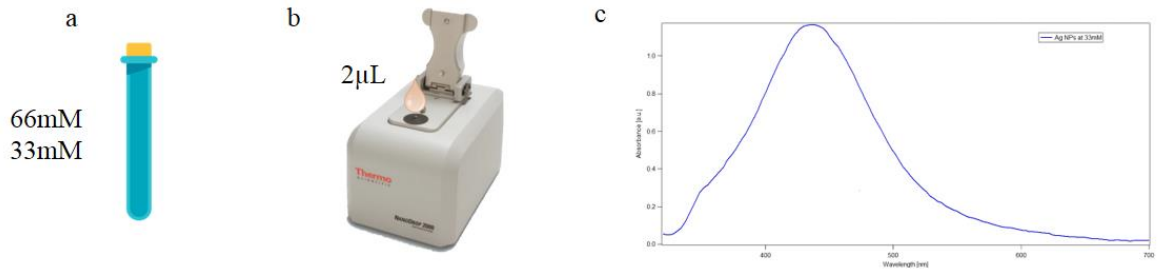

Figure 2.9. Schematic of step-by-step measurement procedure. (a) Resuspension of silver nanoparticles in distillated water at two different concentrations. (b) Place 2µL of sample into the NanoDrop. (c) Typical graph obtained for measurement. The wavelength at which the spectrum shows a maximum is related to the nanoparticle size, assuming spherical nanoparticles.

The data is analyzed using IgorPro (WaveMetrics, OR, USA). The points are measured every 3 nm, which is the error the results will present. The absorbance at the maximum point is shown and the error presented corresponds to the biggest difference between the absorbance measured and the absorbance in the next point. The full width at half maximum (FWHM) is calculated by measuring the difference in wavelength of the points which represent the half of the maximum absorbance value. Only one measurement will be done per sample.

2.2.2 X-ray photoelectron spectroscopy

The equipment used for this analysis is PerkinElmer 1500 XPS system (Hopkinton, MA, USA). As every XPS, ultra-high vacuum conditions must be achieved. For this purpose, two vacuum systems are used. The first one consist in mechanical pumps Turbo-V60 and Turbo-V70 (Varian, CA, USA). The second one is used to achieve ultra-high vacuum conditions, which is the ion getter pump (Perkin Elmer XYZ).

The XPS is used for the analysis of the oxygen, carbon and silver states in the air electrodes before and after each procedure, as shown in Figure 2.10. In this sense, this characterization technique is used to analyze the CNT buckypapers, the impregnation of the silver nanoparticles synthesized by every method over them and the effect each electroanalytical method has over this samples.

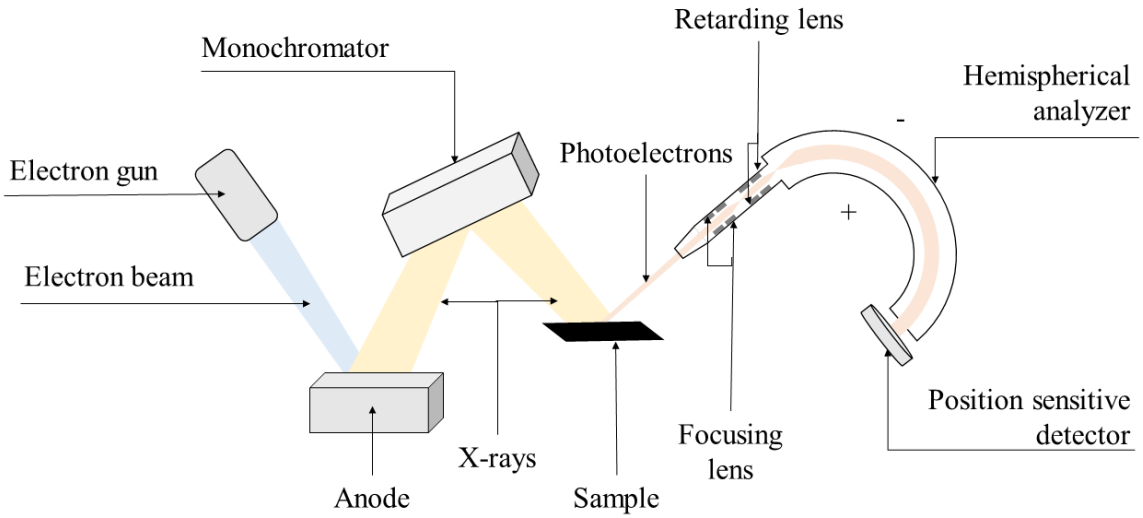

Figure 2.10. Schematic representation of an XPS system
Source: Own elaboration based on C. Cushman, *et al.* Trends in Advanced XPS Instrumentation [85].

The results presented will show the intensity in counts per second (CPS) and the binding energy in electron-volts (eV). First, a general scan of the whole spectrum is taken to identify the elements present in the sample. After that, a high definition scan is done in the regions of interest.

CONCLUSIONS

"The Road goes ever on and on,
Down from the door where it began.
Now far ahead the Road has gone,
And I must follow, if I can,
Pursuing it with eager feet,
Until it joins some larger way
Where many paths and errands meet.
And whither then? I cannot say."

- *J.R.R. Tolkien*

This study stablishes the theoretical framework and scientific support for the development of flexible air cathodes for Zn-air batteries based on CNT buckypapers impregnated with silver nanoparticles and silver nanoparticles with PHF. Silver nanoparticles have shown to be a good catalyst for ORR, as described in literature; therefore, with an adequate impregnation method over a current collector which at the same time acts as support, these nanoparticles should work as part of a suitable air-cathode. Also, due to the similarities between PHF and oxidized carbon materials and the previously reported successful interaction with gold nanoparticles, it is hypothesized that it will act as surfactant for the silver nanoparticle, giving it more stability, and enhanced its catalytic activity. Moreover, it is hypothesized that it can be used as reducing agent for silver nanoparticles synthesis. In order to prove this hypothesis, experimental testing is needed, for which electroanalytical methods like, open circuit potential, cyclic voltammetry and galvanoststic charge-discharge tests are proposed for the evaluation of the performance of the electrode. On the other hand, X-ray photoelectron spectroscopy is proposed for the characterization of the electrodes and UV-vis, for the characterization of the nanoparticles. This study

contributes to the worldwide efforts of the scientific community to develop flexible, small and light batteries and may be a starting point in the use of PHF for this application.

1. Literature review shows challenges in the further development of flexible air cathodes for Zn-air batteries, devices demanded by the market and a good opportunity for technological development in Peru. These challenges can be overcome with novel materials for air cathodes, focused on the enhancement of catalytic activity towards ORR and OER. Different nanoparticle-based materials to be used as air cathodes for Zn-air batteries were evaluated. Among them, CNT buckypaper was selected as suitable as current collector and support for the nanoparticles due to the stability its structure gives, which avoid the nanoparticles to agglomerate silver nanoparticles were selected to be impregnated due to the high ORR catalytic activity shown in literature.
2. A research proposal was developed based on a literature review. Here, it is proposed to use silver nanoparticles supported over CNT buckypaper as air cathodes. Moreover, it is proposed to use PHF as reducing agent in the synthesis of silver nanoparticles and as stabilizing agent for the enhancement of its catalytic activity. On the other hand, experimental tests are proposed for testing the performance of these cathodes. These tests includes Ultraviolet and visible absorption spectroscopy for the characterization of silver nanoparticles, X-ray photoelectron spectroscopy for the characterization of the air-cathode, and open circuit potential, cyclic voltammetry and galvanostatic charge-discharge tests for the performance evaluation.

BIBLIOGRAPHY

[1] Statista, "Wearables sales worldwide by region 2015-2021," 2018. [Online]. Available: https://www.statista.com/statistics/490231/wearable-devices-worldwide-by-region/. [Accessed: 12-Sep-2018].

[2] J. Fu, Z. P. Cano, M. G. Park, A. Yu, M. Fowler, and Z. Chen, "Electrically Rechargeable Zinc-Air Batteries: Progress, Challenges, and Perspectives," *Adv. Mater.*, vol. 29, no. 7, p. 1604685, Feb. 2017.

[3] Q. Liu, Z. Chang, Z. Li, and X. Zhang, "Flexible Metal-Air Batteries: Progress, Challenges, and Perspectives," *Small Methods*, vol. 2, no. 2, p. 1700231, Feb. 2018.

[4] J. Chira Fernández, C. Ríos Moreno, G. Trelles Vásquez, and E. Villarreal Jaramillo, "Estimación del potencial minero metálico del Perú y su contribución económica al Estado, acumulado al 2050," Lima, 2018.

[5] U.S. Department of the Interior, "Historical Statistics for Mineral Commodities in the United States," 2017. [Online]. Available: https://minerals.usgs.gov/minerals/pubs/historical-statistics/. [Accessed: 22-Sep-2018].

[6] M. L. Söderman, D. Kushnir, and B. Sandén, "Will metal scarcity limit the use of electric vehicles?," *Syst. Perspect. Electromobility 2013*, pp. 76–89, 2013.

[7] J.-S. Lee *et al.*, "Metal-Air Batteries with High Energy Density: Li-Air versus Zn-Air," *Adv. Energy Mater.*, vol. 1, no. 1, pp. 34–50, Jan. 2011.

[8] J. Pan, Y. Y. Xu, H. Yang, Z. Dong, H. Liu, and B. Y. Xia, "Advanced Architectures and Relatives of Air Electrodes in Zn-Air Batteries," *Adv. Sci.*, vol. 5, no. 4, p. 1700691, Apr. 2018.

[9] S. Suren and S. Kheawhom, "Development of a High Energy Density Flexible Zinc-Air Battery," *J. Electrochem. Soc.*, vol. 163, no. 6, pp. 846–850, 2016.

[10] A. Sumboja, M. Lübke, Y. Wang, T. An, Y. Zong, and Z. Liu, "All-Solid-State, Foldable, and Rechargeable Zn-Air Batteries Based on Manganese Oxide Grown on Graphene-Coated Carbon Cloth Air Cathode," *Adv. Energy Mater.*, vol. 7, no. 20, p. 1700927, Oct. 2017.

[11] J. Fu *et al.*, "Flexible Rechargeable Zinc-Air Batteries through Morphological Emulation of Human Hair Array," *Adv. Mater.*, vol. 28, no. 30, pp. 6421–6428, Aug. 2016.

[12] D. U. Lee, J. Y. Choi, K. Feng, H. W. Park, and Z. Chen, "Advanced extremely durable 3D bifunctional air electrodes for rechargeable zinc-air batteries," *Adv. Energy Mater.*, vol. 4, no. 6, Apr. 2014.

[13] J. Pan *et al.*, "Recent Progress on Transition Metal Oxides as Bifunctional Catalysts for Lithium-Air and Zinc-Air Batteries," *Batter. Supercaps*, vol. 2, no. 4, pp. 336–347, Apr. 2019.

[14] X. Wu, F. Chen, Y. Jin, N. Zhang, and R. L. Johnston, "Silver–Copper Nanoalloy Catalyst Layer for Bifunctional Air Electrodes in Alkaline Media," *ACS Appl. Mater.*

Interfaces, vol. 7, no. 32, pp. 17782–17791, Aug. 2015.
[15] J. Guo, A. Hsu, D. Chu, and R. Chen, "Improving oxygen reduction reaction activities on carbon-supported Ag nanoparticles in alkaline solutions," *J. Phys. Chem. C*, vol. 114, no. 10, pp. 4324–4330, Mar. 2010.
[16] J. Guo, H. Li, H. He, D. Chu, and R. Chen, "CoPc- and CoPcF16-modified ag nanoparticles as novel catalysts with tunable oxygen reduction activity in alkaline media," *J. Phys. Chem. C*, vol. 115, no. 17, pp. 8494–8502, May 2011.
[17] Y. Jin, F. Chen, Y. Lei, and X. Wu, "A Silver-Copper Alloy as an Oxygen Reduction Electrocatalyst for an Advanced Zinc-Air Battery," *ChemCatChem*, vol. 7, no. 15, pp. 2377–2383, Aug. 2015.
[18] A. Pinedo, B. Alcázar, J. C. Rodriguez-Reyes, A. Pinedo-Flores, and B. Alcázar°, "Protocol for the synthesis of silver nanoparticles using sodium citrate and sodium borohydride as reducing agents," 2018.
[19] M. Gakiya-Teruya, L. Palomino-Marcelo, and J. C. Rodriguez-Reyes, "Synthesis of Highly Concentrated Suspensions of Silver Nanoparticles by Two Versions of the Chemical Reduction Method," *Methods Protoc.*, vol. 2, no. 1, p. 3, Dec. 2018.
[20] R. Das, "Three Hot Trends in Printed and Flexible Electronics," 2017.
[21] H. C. Koydemir and A. Ozcan, "Wearable and Implantable Sensors for Biomedical Applications," *Annu. Rev. Anal. Chem.*, vol. 11, no. 1, pp. 127–146, Jun. 2018.
[22] Y. Khan, A. E. Ostfeld, C. M. Lochner, A. Pierre, and A. C. Arias, "Monitoring of Vital Signs with Flexible and Wearable Medical Devices," *Adv. Mater.*, vol. 28, no. 22, pp. 4373–4395, Jun. 2016.
[23] H. Zhu, Y. Shen, Y. Li, and J. Tang, "Recent advances in flexible and wearable organic optoelectronic devices," *J. Semicond.*, vol. 39, no. 1, p. 011011, Jan. 2018.
[24] D. Ross, M. P. Nemitz, and A. A. Stokes, "Controlling and Simulating Soft Robotic Systems: Insights from a Thermodynamic Perspective."
[25] R. Van Noorden, "The rechargeable revolution: A better battery," *Nature*, vol. 507, no. 7490, pp. 26–28, 2014.
[26] J. W. Choi and D. Aurbach, "Promise and reality of post-lithium-ion batteries with high energy densities," *Nature Reviews Materials*, vol. 1, no. 4. Nature Publishing Group, pp. 1–16, 31-Mar-2016.
[27] F. Rojas, V. Garay, and J. Cantallopts, "Mercado internacional del litio y su potencial en Chile," 2018.
[28] D. Desormeaux, "Litio: Mercado y Regulación en Chile Daniela Desormeaux-Socia y Gerente General-signumBOX Inteligencia de Mercados EXPOMIN," 2018.
[29] N. J. Tro, *Chemistry : a molecular approach*, 3rd ed. Pearson, 2013.
[30] T. L. Brown, H. E. Lemay, B. E. Bursten, C. J. Murphy, and P. M. Woodward, *Chemistry-The-Central-Science-in-SI-Units-global-edition-14th-ed-*. 2017.
[31] V. S. Bagotsky and A. N. Frumkin, *Fundamentals of Electrochemistry*. 2006.
[32] OpenStax, "Chemistry." .
[33] T. Stoebe, "Classification of Cells or Batteries," *University of Washington*, 2000. [Online]. Available: https://depts.washington.edu/matseed/batteries/MSE/classification.html. [Accessed: 27-Nov-2018].
[34] Battery Association of Japan, "BAJ Website | Monthly battery sales statistics," 2018.

[Online]. Available: http://www.baj.or.jp/e/statistics/02.php. [Accessed: 27-Nov-2018].
[35] EPEC, “Primary and Rechargeable Battery Chemistries with Energy Density,” 2018. [Online]. Available: https://www.epectec.com/batteries/chemistry/. [Accessed: 28-Nov-2018].
[36] T. B. Reddy and D. Linden, *Linden’s handbook of batteries*. McGraw-Hill, 2011.
[37] R. Putt, N. Naimer, B. Koretz, and T. Atwater, “Advanced Zinc-Air Primary Batteries,” in *39th Power Sources Conference*, 2000.
[38] M. G. Park, D. U. Lee, M. H. Seo, Z. P. Cano, and Z. Chen, “3D Ordered Mesoporous Bifunctional Oxygen Catalyst for Electrically Rechargeable Zinc-Air Batteries,” *Small*, vol. 12, no. 20, pp. 2707–2714, May 2016.
[39] D. U. Lee, M. G. Park, H. W. Park, M. H. Seo, X. Wang, and Z. Chen, “Highly Active and Durable Nanocrystal-Decorated Bifunctional Electrocatalyst for Rechargeable Zinc-Air Batteries,” *ChemSusChem*, vol. 8, no. 18, pp. 3129–3138, Sep. 2015.
[40] W. E. Org, W. Hong, H. Li, and B. Wang, “ELECTROCHEMICAL SCIENCE A Horizontal Three-Electrode Structure for Zinc-Air Batteries with Long-Term Cycle Life and High Performance,” *Int. J. Electrochem. Sci*, vol. 11, pp. 3843–3851, 2016.
[41] S. Amendola *et al.*, “Electrically rechargeable, metal-air battery systems and methods,” 20-Jul-2011.
[42] S. Smedley, B. Wozniczka, and D. R. Bruce, “Metal-air fuel cell,” 13-Sep-2016.
[43] J. Fu *et al.*, “Defect Engineering of Chalcogen-Tailored Oxygen Electrocatalysts for Rechargeable Quasi-Solid-State Zinc-Air Batteries,” *Adv. Mater.*, vol. 29, no. 35, p. 1702526, Sep. 2017.
[44] Q. Liu, Y. Wang, L. Dai, and J. Yao, “Scalable Fabrication of Nanoporous Carbon Fiber Films as Bifunctional Catalytic Electrodes for Flexible Zn-Air Batteries,” *Adv. Mater.*, vol. 28, no. 15, pp. 3000–3006, Apr. 2016.
[45] S. Li, Z. P. Guo, C. Y. Wang, G. G. Wallace, and H. K. Liu, “Flexible cellulose based polypyrrole–multiwalled carbon nanotube films for bio-compatible zinc batteries activated by simulated body fluids,” *J. Mater. Chem. A*, vol. 1, no. 45, p. 14300, Oct. 2013.
[46] J. Park, M. Park, G. Nam, J. Lee, and J. Cho, “All-Solid-State Cable-Type Flexible Zinc-Air Battery,” *Adv. Mater.*, vol. 27, no. 8, pp. 1396–1401, Feb. 2015.
[47] Y. Li and H. Dai, “Recent advances in zinc–air batteries,” *Chem. Soc. Rev.*, vol. 43, no. 15, pp. 5257–5275, Jul. 2014.
[48] K. Wang *et al.*, “Dendrite growth in the recharging process of zinc–air batteries,” *J. Mater. Chem. A*, vol. 3, no. 45, pp. 22648–22655, Nov. 2015.
[49] H. Yang, H. Zhang, X. Wang, J. Wang, X. Meng, and Z. Zhou, “Calcium Zincate Synthesized by Ballmilling as a Negative Material for Secondary Alkaline Batteries,” *J. Electrochem. Soc.*, vol. 151, no. 12, p. A2126, Dec. 2004.
[50] J. Huang, Z. Yang, R. Wang, Z. Zhang, Z. Feng, and X. Xie, “Zn–Al layered double oxides as high-performance anode materials for zinc-based secondary battery,” *J. Mater. Chem. A*, vol. 3, no. 14, pp. 7429–7436, Mar. 2015.
[51] D. U. Lee, J. Fu, M. G. Park, H. Liu, A. Ghorbani Kashkooli, and Z. Chen, “Self-Assembled NiO/Ni(OH) 2 Nanoflakes as Active Material for High-Power and High-Energy Hybrid Rechargeable Battery,” *Nano Lett.*, vol. 16, no. 3, pp. 1794–1802, Mar.

2016.
[52] J. Fu *et al.*, “A flexible solid-state electrolyte for wide-scale integration of rechargeable zinc–air batteries,” *Energy Environ. Sci.*, vol. 9, no. 2, pp. 663–670, Feb. 2016.
[53] FuelCellsEtc, “Commercial Fuel Cell Components Gas Diffusion Layer (GDL),” 2017.
[54] Z. Ma *et al.*, “Degradation characteristics of air cathode in zinc air fuel cells,” *J. Power Sources*, vol. 274, pp. 56–64, Jan. 2015.
[55] L. Li, Z. Chang, and X.-B. Zhang, “Recent Progress on the Development of Metal-Air Batteries,” *Adv. Sustain. Syst.*, vol. 1, no. 10, p. 1700036, Oct. 2017.
[56] C. Lai, P. Kolla, Y. Zhao, H. Fong, and A. L. Smirnova, “Lignin-derived electrospun carbon nanofiber mats with supercritically deposited Ag nanoparticles for oxygen reduction reaction in alkaline fuel cells,” *Electrochim. Acta*, vol. 130, pp. 431–438, Jun. 2014.
[57] H. Erikson, A. Sarapuu, and K. Tammeveski, “Oxygen Reduction Reaction on Silver Catalysts in Alkaline Media: a Minireview,” *ChemElectroChem*, vol. 6, no. 1, pp. 73–86, Jan. 2019.
[58] T. M. D. Dang, T. T. T. Le, E. Fribourg-Blanc, and M. C. Dang, “Influence of surfactant on the preparation of silver nanoparticles by polyol method,” *Adv. Nat. Sci. Nanosci. Nanotechnol.*, vol. 3, no. 3, Sep. 2012.
[59] E. M. Egorova, A. A. Kubatiev, and V. I. Schvets, *Biological effects of metal nanoparticles*. Springer International Publishing, 2016.
[60] Y. Wang and Y. Xia, “Bottom-up and top-down approaches to the synthesis of monodispersed spherical colloids of low melting-point metals,” *Nano Lett.*, vol. 4, no. 10, pp. 2047–2050, Oct. 2004.
[61] Z. Khan, S. A. Al-Thabaiti, A. Y. Obaid, and A. O. Al-Youbi, “Preparation and characterization of silver nanoparticles by chemical reduction method,” *Colloids Surfaces B Biointerfaces*, vol. 82, no. 2, pp. 513–517, Feb. 2011.
[62] L. Kvítek *et al.*, “Effect of surfactants and polymers on stability and antibacterial activity of silver nanoparticles (NPs),” *J. Phys. Chem. C*, vol. 112, no. 15, pp. 5825–5834, Apr. 2008.
[63] P. M. Luis Alberto, “Evaluación de la interacción de nanopartículas de plata con factor de crecimiento epidermal para su uso potencial en sistemas que mejoren la regeneración de tejidos epiteliales,” Universidad Nacional Mayor de San Marcos, 2019.
[64] T. A. Skipa and V. K. Koltover, “Fullerene Trend in Biomedicine: Expectations and Reality.” 2019.
[65] J. Gao *et al.*, “Polyhydroxy fullerenes (fullerols or fullerenols): beneficial effects on growth and lifespan in diverse biological models.,” *PLoS One*, vol. 6, no. 5, p. e19976, 2011.
[66] V. Krishna *et al.*, “Contaminant-Activated Visible Light Photocatalysis,” *Sci. Rep.*, vol. 8, no. 1, Dec. 2018.
[67] K. Kokubo, M. K. E. Cabbello, N. Sato, Y. Uetake, and H. Sakurai, “Gold Nanoparticles Stabilized by Molecular Fullerenols,” *ChemNanoMat*, p. cnma.201900778, Feb. 2020.

[68] R. Ciganda *et al.*, “Gold nanoparticles as electron reservoir redox catalysts for 4-nitrophenol reduction: A strong stereoelectronic ligand influence,” *Chem. Commun.*, vol. 50, no. 70, pp. 10126–10129, Sep. 2014.
[69] M. T. Islam *et al.*, “Fullerene stabilized gold nanoparticles supported on titanium dioxide for enhanced photocatalytic degradation of methyl orange and catalytic reduction of 4-nitrophenol,” *J. Environ. Chem. Eng.*, vol. 6, no. 4, pp. 3827–3836, Aug. 2018.
[70] A. W. Czanderna and D. M. Hercules, Eds., *Ion Spectroscopies for Surface Analysis*. Boston, MA: Springer US, 1991.
[71] J. C. Zamarripa Rodríguez, “La constante de Planck.”
[72] J. W. Niemantsverdriet, *Spectroscopy in catalysis : an introduction*. VCH, 1995.
[73] D. A. Skoog, D. M. West, F. J. Holler, and S. R. Crouch, *Fundamentals of analytical chemistry*. .
[74] C. De Caro, “UV / VIS Spectrophotometry,” *Mettler-Toledo Int.*, no. September 2015, pp. 4–14, 2015.
[75] R. Desai, V. Mankad, S. K. Gupta, and P. K. Jha, “Size distribution of silver nanoparticles: UV-visible spectroscopic assessment,” *Nanosci. Nanotechnol. Lett.*, vol. 4, no. 1, pp. 30–34, 2012.
[76] P. W. (Peter W. Atkins and J. De Paula, *Physical chemistry*. W.H. Freeman and Co, 2010.
[77] N. N. Elgrishi, K. J. Rountree, B. D. Mccarthy, E. S. Rountree, T. T. Eisenhart, and J. L. Dempsey, “A Practical Beginner’s Guide to Cyclic Voltammetry,” 2017.
[78] V. Knap *et al.*, “Reference Performance Test Methodology for Degradation Assessment of Lithium-Sulfur Batteries,” *J. Electrochem. Soc.*, vol. 165, no. 9, pp. A1601–A1609, Jan. 2018.
[79] KEITHLEY, “Rechargeable Battery Charge/Discharge Cycling Using the Keithley Model 2450 SourceMeter ® SMU Instrument,” 2013.
[80] MIT Electric Vehicle Team, “A Guide to Understanding Battery Specifications,” 2008.
[81] C. J. Zhong, N. T. Woods, G. B. Dawson, and M. D. Porter, “Formation of thiol-based monolayers on gold: Implications from open circuit potential measurements,” *Electrochem. commun.*, vol. 1, no. 1, pp. 17–21, Jan. 1999.
[82] M. J. Avena, O. R. Cámara, and C. P. De Pauli, “Open circuit potential measurements with Ti/TiO2 electrodes,” *Colloids and Surfaces*, vol. 69, no. 4, pp. 217–228, Jan. 1993.
[83] Y. Liang *et al.*, “Co3O4 nanocrystals on graphene as a synergistic catalyst for oxygen reduction reaction,” *Nat. Mater.*, vol. 10, no. 10, pp. 780–786, 2011.
[84] Y. Wang, Y. Song, and Y. Xia, “Electrochemical capacitors: Mechanism, materials, systems, characterization and applications,” *Chemical Society Reviews*, vol. 45, no. 21. Royal Society of Chemistry, pp. 5925–5950, 07-Nov-2016.
[85] C. Cushman, S. Chatterjee, G. H. Major, N. J. Smith, A. J. Roberts, and M. R. Linford, “Trends in Advanced XPS Instrumentation. 1. Overview of the Technique, Automation, High Sensitivity, Imaging, Snapshot Spectroscopy, Gas Cluster Ion Beams, and Multiple Analytical Techniques on the Instrument.” p. 8, 2016.
[86] Y. Jin and F. Chen, “Facile preparation of Ag-Cu bifunctional electrocatalysts for zinc-

air batteries," *Electrochim. Acta*, vol. 158, pp. 437–445, Mar. 2015.
[87] J. Hu, Z. Shi, X. Wang, H. Qiao, and H. Huang, "Silver-modified porous 3D nitrogen-doped graphene aerogel: Highly efficient oxygen reduction electrocatalyst for Zn−Air battery," *Electrochim. Acta*, vol. 302, pp. 216–224, Apr. 2019.
[88] Q. Wang, H. Miao, S. Sun, Y. Xue, and Z. Liu, "One-Pot Synthesis of Co3O4/Ag Nanoparticles Supported on N-Doped Graphene as Efficient Bifunctional Oxygen Catalysts for Flexible Rechargeable Zinc–Air Batteries," *Chem. - A Eur. J.*, vol. 24, no. 55, pp. 14816–14823, Oct. 2018.
[89] F. W. T. Goh, Z. Liu, X. Ge, Y. Zong, G. Du, and T. S. A. Hor, "Ag nanoparticle-modified MnO 2 nanorods catalyst for use as an air electrode in zinc-air battery," *Electrochim. Acta*, vol. 114, pp. 598–604, 2013.

ANNEXES

ANNEX 1: Zn-air batteries with Ag-based catalysts

Bifunctional air electrode	Synthesis method	Cell components	Performance	Ref.
AgCu on Ni foam	Electrochemical deposition	Zn/6M KOH + 0.2M $Zn(OAc)_2$	86.5 mW cm^{-2} @ 100 mA cm^{-2}, round efficiency of 56.4% @ 20 mA cm^{-2}	[17]
AgCu on Ni foam	Galvanic displacement on Ni-foam	Zn plate/6M KOH + 0.2M Zinc acetate	85.8 mW cm^{-2} @ 100 mA cm^{-2}, 572 mAh g^{-1} normalized by Zn anode consumed, 53.08% after 100 cycles	[86]
Ag on 3D N-doped graphene	One-step hydrothermal method	Zn plate/KOH	29.8 mW cm^{-2} @ 100 mA cm^{-2}	[87]
Co_3O_4/Ag on N-reduced graphene	One-pot solvothermal method	Zn foil/polyacrylic acid-based gel-electrolyte	108 mW cm^{-2} @ ~175 mA cm^{-2}, charge-discharge gap after 100 cycles are 0.77 V	[88]
$Ag_{50}Cu_{50}$ on Ni foam	Pulsed layer deposition	Zn plate/6M KOH + 0.1M $Zn(CH_3COO)_2$	45.1 mW cm-2 @ 100 mA cm^{-2}, ~50% efficiency @ 20 mA cm^{-2}	[14]
Ag-αMnO_2	Microwave-assisted polyol method	Zn plate/6M KOH	Battery voltage sustained after 270 cycles	[89]

Table 0.1. Zn-air batteries with Ag-based catalysts and their performances.